



**HAL**  
open science

## Vulnerability of mineral-associated soil organic carbon to climate across global drylands

Paloma Díaz-Martínez, Fernando Maestre, Eduardo Moreno-Jiménez, Manuel Delgado-Baquerizo, David Eldridge, Hugo Saiz, Nicolas Gross, Yoann Le Bagousse-Pinguet, Beatriz Gozalo, Victoria Ochoa, et al.

### ► To cite this version:

Paloma Díaz-Martínez, Fernando Maestre, Eduardo Moreno-Jiménez, Manuel Delgado-Baquerizo, David Eldridge, et al.. Vulnerability of mineral-associated soil organic carbon to climate across global drylands. *Nature Climate Change*, 2024, 14 (9), pp.976-982. 10.1038/s41558-024-02087-y . hal-04735409

**HAL Id: hal-04735409**

**<https://hal.science/hal-04735409v1>**

Submitted on 14 Oct 2024

**HAL** is a multi-disciplinary open access archive for the deposit and dissemination of scientific research documents, whether they are published or not. The documents may come from teaching and research institutions in France or abroad, or from public or private research centers.

L'archive ouverte pluridisciplinaire **HAL**, est destinée au dépôt et à la diffusion de documents scientifiques de niveau recherche, publiés ou non, émanant des établissements d'enseignement et de recherche français ou étrangers, des laboratoires publics ou privés.

25 **Vulnerability of mineral-associated soil organic carbon to climate across**  
26 **global drylands**

27

28 Paloma Díaz-Martínez<sup>1</sup>, Fernando T. Maestre<sup>2</sup>, Eduardo Moreno-Jiménez<sup>3,4</sup>, Manuel Delgado-  
29 Baquerizo<sup>5</sup>, David J. Eldridge<sup>6</sup>, Hugo Saiz<sup>7</sup>, Nicolas Gross<sup>8</sup>, Yoann Le Bagousse-Pinguel<sup>9</sup>,  
30 Beatriz Gozalo<sup>10</sup>, Victoria Ochoa<sup>1,10</sup>, Emilio Guirado<sup>10</sup>, Miguel García-Gómez<sup>11</sup>, Enrique  
31 Valencia<sup>12</sup>, Sergio Asensio<sup>10</sup>, Miguel Berdugo<sup>12</sup>, Jaime Martínez-Valderrama<sup>10,13</sup>, Betty J.  
32 Mendoza<sup>14</sup>, Juan C. García-Gil<sup>1</sup>, Claudio Zaccone<sup>15</sup>, Marco Panettieri<sup>1</sup>, Pablo García-  
33 Palacios<sup>1,16</sup>, Wei Fan<sup>17</sup>, Iria Benavente-Ferraces<sup>1</sup>, Ana Rey<sup>18</sup>, Nico Eisenhauer<sup>19,20</sup>, Simone  
34 Cesarz<sup>19,20</sup>, Mehdi Abedi<sup>21</sup>, Rodrigo J. Ahumada<sup>22</sup>, Julio M. Alcántara<sup>23</sup>, Fateh Amghar<sup>24</sup>,  
35 Valeria Aramayo<sup>25</sup>, Antonio I. Arroyo<sup>26</sup>, Khadijeh Bahalkeh<sup>21</sup>, Farah Ben Salem<sup>27</sup>, Niels  
36 Blaum<sup>28</sup>, Bazartseren Boldgiv<sup>29</sup>, Matthew A. Bowker<sup>30,31</sup>, Donaldo Bran<sup>25</sup>, Cristina  
37 Branquinho<sup>32</sup>, Chongfeng Bu<sup>33</sup>, Yonatan Cáceres<sup>34</sup>, Rafaella Canessa<sup>35,19,36</sup>, Andrea P. Castillo-  
38 Monroy<sup>37</sup>, Ignacio Castro<sup>38</sup>, Patricio Castro-Quezada<sup>39</sup>, Roukaya Chibani<sup>40</sup>, Abel A.  
39 Conceição<sup>41</sup>, Courtney M. Currier<sup>42</sup>, Anthony Darrouzet-Nardi<sup>43</sup>, Balázs Deák<sup>44</sup>, Christopher R.  
40 Dickman<sup>45</sup>, David A. Donoso<sup>37</sup>, Andrew J. Dougill<sup>46</sup>, Jorge Durán<sup>47</sup>, Hamid Ejtehadi<sup>48</sup>, Carlos  
41 Espinosa<sup>49</sup>, Alex Fajardo<sup>50</sup>, Mohammad Farzam<sup>51,52</sup>, Daniela Ferrante<sup>53,54</sup>, Lauchlan H. Fraser<sup>55</sup>,  
42 Juan J. Gaitán<sup>56,57</sup>, Elizabeth Gusman Montalván<sup>49</sup>, Rosa M. Hernández-Hernández<sup>38</sup>, Andreas  
43 von Hessberg<sup>58</sup>, Norbert Hölzel<sup>59</sup>, Elisabeth Huber-Sannwald<sup>60</sup>, Frederic M. Hughes<sup>61,41,62</sup>,  
44 Oswaldo Jadán-Maza<sup>39</sup>, Katja Geissler<sup>28</sup>, Anke Jentsch<sup>58</sup>, Mengchen Ju<sup>33,63</sup>, Kudzai F. Kaseke<sup>64</sup>,  
45 Liana Kindermann<sup>65</sup>, Jessica E. Koopman<sup>66</sup>, Peter C. Le Roux<sup>67</sup>, Pierre Liancourt<sup>68,36</sup>, Anja  
46 Linstädter<sup>65,69</sup>, Jushan Liu<sup>70</sup>, Michelle A. Louw<sup>67</sup>, Gillian Maggs-Kölling<sup>71</sup>, Thulani P.  
47 Makhalanyane<sup>72</sup>, Oumarou Malam Issa<sup>73</sup>, Eugene Marais<sup>71</sup>, Pierre Margerie<sup>74</sup>, Antonio J.  
48 Mazaneda<sup>75</sup>, Mitchel P. McClaran<sup>76</sup>, João Vitor S. Messeder<sup>77</sup>, Juan P. Mora<sup>78</sup>, Gerardo  
49 Moreno<sup>34</sup>, Seth M. Munson<sup>79</sup>, Alice Nunes<sup>32</sup>, Gabriel Oliva<sup>53,54</sup>, Gastón R. Oñatibia<sup>80</sup>, Brooke  
50 Osborne<sup>81</sup>, Guadalupe Peter<sup>56,82</sup>, Yolanda Pueyo<sup>26</sup>, R. Emiliano Quiroga<sup>22,83</sup>, Sasha C. Reed<sup>84</sup>,  
51 Victor M. Reyes<sup>85</sup>, Alexandra Rodríguez<sup>47</sup>, Jan C. Ruppert<sup>36</sup>, Oswaldo Sala<sup>86,87,88</sup>, Ayman  
52 Salah<sup>89</sup>, Julius Sebei<sup>90</sup>, Michael Sloan<sup>30</sup>, Shijirbaatar Solongo<sup>91</sup>, Ilan Stavi<sup>92</sup>, Colton R.A.  
53 Stephens<sup>55</sup>, Alberto L. Teixido<sup>12</sup>, Andrew D. Thomas<sup>93</sup>, Heather L. Throop<sup>94,86</sup>, Katja  
54 Tielbörger<sup>36</sup>, Samantha Travers<sup>6</sup>, James Val<sup>95</sup>, Orsolya Valko<sup>44</sup>, Liesbeth van den Brink<sup>36,96</sup>,  
55 Frederike Velbert<sup>59</sup>, Wanyoike Wamiti<sup>97</sup>, Deli Wang<sup>70</sup>, Lixin Wang<sup>98</sup>, Glenda M. Wardle<sup>45</sup>,  
56 Laura Yahdjian<sup>80</sup>, Eli Zaady<sup>99,100</sup>, Juan M. Zeberio<sup>82</sup>, Yuanming Zhang<sup>101</sup>, Xiaobing Zhou<sup>101</sup>,  
57 César Plaza<sup>1</sup>

58

59 <sup>1</sup>Instituto de Ciencias Agrarias (ICA), CSIC, Madrid, Spain. <sup>2</sup>Environmental Sciences and  
60 Engineering, Biological and Environmental Science and Engineering Division, King Abdullah  
61 University of Science and Technology, Thuwal, Kingdom of Saudi Arabia. <sup>3</sup>Department of  
62 Agricultural and Food Chemistry, Faculty of Sciences, Universidad Autónoma de Madrid,  
63 Madrid, Spain. <sup>4</sup>Institute for Advanced Research in Chemical Sciences, Madrid, Spain.

64 <sup>5</sup>Laboratorio de Biodiversidad y Funcionamiento Ecosistémico, Instituto de Recursos Naturales y  
65 Agrobiología de Sevilla (IRNAS), CSIC, Sevilla, Spain. <sup>6</sup>Centre for Ecosystem Science, School  
66 of Biological, Earth and Environmental Sciences, University of New South Wales, Sydney, New

67 South Wales, Australia. <sup>7</sup>Departamento de Ciencias Agrarias y Medio Natural, Escuela  
68 Politécnica Superior, Instituto Universitario de Investigación en Ciencias Ambientales de Aragón  
69 (IUCA), Universidad de Zaragoza, Huesca, Spain. <sup>8</sup>Université Clermont Auvergne, INRAE,  
70 VetAgro Sup, Unité Mixte de Recherche Ecosystème Prairial, Clermont-Ferrand, France. <sup>9</sup>Aix  
71 Marseille Univ, CNRS, Avignon Université, IRD, IMBE, Aix-en-Provence, France. <sup>10</sup>Instituto  
72 Multidisciplinar para el Estudio del Medio "Ramón Margalef", Universidad de Alicante,  
73 Alicante, Spain. <sup>11</sup>Departamento de Ingeniería y Morfología del Terreno, Escuela Técnica  
74 Superior de Ingenieros de Caminos, Canales y Puertos, Universidad Politécnica de Madrid,  
75 Madrid, Spain. <sup>12</sup>Departamento de Biodiversidad, Ecología y Evolución, Facultad de Ciencias  
76 Biológicas, Universidad Complutense de Madrid, Madrid, Spain. <sup>13</sup>Estación Experimental de  
77 Zonas Áridas (EEZA), CSIC, Almería, Spain. <sup>14</sup>Departamento de Biología y Geología, Física y  
78 Química Inorgánica, Universidad Rey Juan Carlos, Madrid, Spain. <sup>15</sup>Department of  
79 Biotechnology, University of Verona, Verona, Italy. <sup>16</sup>Department of Plant and Microbial  
80 Biology, University of Zurich, Zurich, Switzerland. <sup>17</sup>Institute of Agricultural Environment and  
81 Resources, Jilin Academy of Agricultural Sciences, Changchun, China. <sup>18</sup>Museo Nacional de  
82 Ciencias Naturales (MNCN), CSIC, Madrid, Spain. <sup>19</sup>German Centre for Integrative Biodiversity  
83 Research (iDiv) Halle-Jena-Leipzig, Leipzig, Germany. <sup>20</sup>Leipzig University, Institute of  
84 Biology, Leipzig, Germany. <sup>21</sup>Department of Range Management, Faculty of Natural Resources  
85 and Marine Sciences, Tarbiat Modares University, Noor, Mazandaran Province, Iran. <sup>22</sup>Instituto  
86 Nacional de Tecnología Agropecuaria, Estación Experimental Agropecuaria Catamarca,  
87 Catamarca, Argentina. <sup>23</sup>Instituto Interuniversitario de Investigación del Sistema Tierra en  
88 Andalucía, Universidad de Jaén, Jaén, Spain. <sup>24</sup>Laboratoire de Recherche: Biodiversité,  
89 Biotechnologie, Environnement et Développement Durable (BioDev), Faculté des Sciences,  
90 Université M'hamed Bougara de Boumerdès, Boumerdès, Algérie. <sup>25</sup>Instituto Nacional de  
91 Tecnología Agropecuaria, Estación Experimental Agropecuaria Bariloche, Bariloche, Río Negro,  
92 Argentina. <sup>26</sup>Instituto Pirenaico de Ecología (IPE), CSIC, Zaragoza, Spain. <sup>27</sup>Laboratory of  
93 Pastoral Ecosystems and Promotion of Spontaneous plants and Associated Microorganisms,  
94 Institut des Régions Arides (IRA) Médenine, Tunisia. <sup>28</sup>University of Potsdam, Plant Ecology  
95 and Nature Conservation, Potsdam, Germany. <sup>29</sup>Laboratory of Ecological and Evolutionary  
96 Synthesis, Department of Biology, School of Arts and Sciences, National University of  
97 Mongolia, Ulaanbaatar, Mongolia. <sup>30</sup>School of Forestry, Northern Arizona University, Flagstaff,  
98 AZ, USA. <sup>31</sup>Center for Ecosystem Science and Society, Northern Arizona University, Flagstaff,  
99 AZ, USA. <sup>32</sup>Center for Ecology, Evolution and Environmental Changes (cE3c) & CHANGE -  
100 Global Change and Sustainability Institute, Faculdade de Ciências, Universidade de Lisboa,  
101 Campo Grande, Lisboa, Portugal. <sup>33</sup>Institute of Soil and Water Conservation, Northwest  
102 Agriculture and Forestry University, Yangling, Shaanxi, China. <sup>34</sup>Forestry School, INDEHESA,  
103 Universidad de Extremadura, Plasencia, Spain. <sup>35</sup>Institute of Biology, Martin Luther University  
104 Halle-Wittenberg, Halle, Germany. <sup>36</sup>Plant Ecology Group, University of Tübingen, Tübingen,  
105 Germany. <sup>37</sup>Grupo de Investigación en Ecología y Evolución en los Trópicos-EE Trop-  
106 Universidad de las Américas, Campus Udlapark, Quito, Ecuador. <sup>38</sup>Universidad Nacional  
107 Experimental Simón Rodríguez (UNESR), Instituto de Estudios Científicos y Tecnológicos  
108 (IDECYT), Centro de Estudios de Agroecología Tropical (CEDAT), Laboratorio de  
109 Biogeoquímica, Miranda, Venezuela. <sup>39</sup>Grupo de Ecología Forestal y Agroecosistemas, Facultad  
110 de Ciencias Agropecuarias, Universidad de Cuenca, Cuenca, Ecuador. <sup>40</sup>Laboratory of  
111 Eremology and Combating Desertification; Institut des Régions Arides (IRA), Médenine,  
112 Tunisia. <sup>41</sup>Universidade Estadual de Feira de Santana, Departamento de Ciências Biológicas,

113 Feira de Santana, Bahia, Brazil. <sup>42</sup>Department of Plant Sciences, University of Cambridge,  
114 Cambridge, UK. <sup>43</sup>Department of Biological Sciences, University of Texas at El Paso, El Paso,  
115 TX, USA. <sup>44</sup>Lendület Seed Ecology Research Group, Institute of Ecology and Botany, HUN-  
116 REN Centre for Ecological Research, Vácrátót, Hungary. <sup>45</sup>Desert Ecology Research Group,  
117 School of Life and Environmental Sciences, The University of Sydney, Sydney, New South  
118 Wales, Australia. <sup>46</sup>School of Earth and Environment, University of Leeds, Leeds, UK. <sup>47</sup>Misión  
119 Biológica de Galicia (MBG), CSIC, Pontevedra, Spain. <sup>48</sup>Quantitative Plant Ecology and  
120 Biodiversity Research Lab., Department of Biology, Faculty of Science, Ferdowsi University of  
121 Mashhad, Mashhad, Iran. <sup>49</sup>Departamento de Ciencias Biológicas, Universidad Técnica  
122 Particular de Loja, Loja, Ecuador. <sup>50</sup>Instituto de Investigación Interdisciplinaria (I3), Universidad  
123 de Talca, Talca, Chile. <sup>51</sup>Department of Range and Watershed Management, Ferdowsi University  
124 of Mashhad, Mashhad, Iran. <sup>52</sup>Department of Molecular and Life Sciences, Curtin University,  
125 Australia. <sup>53</sup>Universidad Nacional de la Patagonia Austral, Río Gallegos, Santa Cruz, Argentina.  
126 <sup>54</sup>Instituto Nacional de Tecnología Agropecuaria, Estación Experimental Agropecuaria Santa  
127 Cruz, Santa Cruz, Argentina. <sup>55</sup>Department of Natural Resource Science, Thompson Rivers  
128 University, British Columbia, Canada. <sup>56</sup>Consejo Nacional de Investigaciones Científicas y  
129 Técnicas de Argentina (CONICET), Buenos Aires, Argentina. <sup>57</sup>Departamento de Tecnología,  
130 Universidad Nacional de Luján, Buenos Aires, Argentina. <sup>58</sup>Department of Disturbance Ecology,  
131 Bayreuth Center of Ecology and Environmental Research BayCEER, University of Bayreuth,  
132 Bayreuth, Germany. <sup>59</sup>Institute of Landscape Ecology, University of Münster, Münster,  
133 Germany. <sup>60</sup>Instituto Potosino de Investigación Científica y Tecnológica, A.C., SLP, Mexico.  
134 <sup>61</sup>Universidade Estadual de Santa Cruz, Conselho de Curadores das Coleções Científicas and  
135 Zoologia, Ilhéus, Bahia, Brazil. <sup>62</sup>Universidade Federal de Minas Gerais, Bioinformática, Belo  
136 Horizonte, Minas Gerais, Brazil. <sup>63</sup>Yangling Vocational & Technical College, Yangling,  
137 Shaanxi, China. <sup>64</sup>Earth Research Institute, University of California Santa Barbara, CA, USA.  
138 <sup>65</sup>University of Potsdam, Institute of Biochemistry and Biology, Biodiversity Research /  
139 Systematic Botany, Potsdam, Germany. <sup>66</sup>Centre for Microbial Ecology and Genomics,  
140 Department of Biochemistry, Genetics and Microbiology, University of Pretoria, Pretoria, South  
141 Africa. <sup>67</sup>Department of Plant and Soil Sciences, University of Pretoria, Pretoria, South Africa.  
142 <sup>68</sup>Institute Botany Department, State Museum of Natural History Stuttgart, Stuttgart, Germany.  
143 <sup>69</sup>Institute of Crop Science and Resource Conservation, University of Bonn, Bonn, Germany.  
144 <sup>70</sup>Key Laboratory of Vegetation Ecology of the Ministry of Education, Jilin Songnen Grassland  
145 Ecosystem National Observation and Research Station, Institute of Grassland Science, Northeast  
146 Normal University, Changchun, China. <sup>71</sup>Gobabeb-Namib Research Institute, Walvis Bay,  
147 Namibia. <sup>72</sup>Department of Microbiology and the School of Data Science and Computational  
148 Thinking, Faculty of Science, Stellenbosch University, Stellenbosch, South Africa. <sup>73</sup>Institut  
149 d'Écologie et des Sciences de l'Environnement de Paris (iEES-Paris), Sorbonne Université, IRD,  
150 CNRS, INRAE, Université Paris Est Creteil, Université de Paris, France. <sup>74</sup>Normandie Univ,  
151 UNIROUEN, INRAE, ECODIV, Rouen, France. <sup>75</sup>Departamento de Biología Animal, Biología  
152 Vegetal y Ecología, Universidad de Jaén, Jaén, Spain. <sup>76</sup>School of Natural Resources and the  
153 Environment, University of Arizona, Tucson, AZ, USA. <sup>77</sup>Biology Department & Ecology  
154 Program, The Pennsylvania State University, University Park, PA, USA. <sup>78</sup>Doctoral Program in  
155 Sciences mention in Plant Biology and Biotechnology, Institute of Biological Sciences, Campus  
156 Talca, Universidad de Talca, Chile. <sup>79</sup>US Geological Survey, Southwest Biological Science  
157 Center, Flagstaff, AZ, USA. <sup>80</sup>Cátedra de Ecología, Facultad de Agronomía, Universidad de  
158 Buenos Aires, Instituto de Investigaciones Fisiológicas y Ecológicas Vinculadas a la Agricultura

159 (IFEVA-CONICET), Buenos Aires, Argentina. <sup>81</sup>Department of Environment and Society, Utah  
160 State University, Moab, UT, USA. <sup>82</sup>Universidad Nacional de Río Negro, Sede Atlántica,  
161 CEANPa, Río Negro, Argentina. <sup>83</sup>Cátedra de Manejo de Pastizales Naturales, Facultad de  
162 Ciencias Agrarias, Universidad Nacional de Catamarca, Catamarca, Argentina. <sup>84</sup>US Geological  
163 Survey, Southwest Biological Science Center, Moab, UT, USA. <sup>85</sup>Instituto de Ecología,  
164 INECOL, Chihuahua, Chihuahua, Mexico. <sup>86</sup>School of Life Sciences, Arizona State University,  
165 Tempe, AZ, USA. <sup>87</sup>School of Sustainability, Arizona State University, Tempe, AZ, USA.  
166 <sup>88</sup>Global Drylands Center, Arizona State University, Tempe, AZ, USA. <sup>89</sup>Al-Quds University,  
167 Palestine. <sup>90</sup>Department of Agriculture, Makhado, Limpopo, South Africa. <sup>91</sup>Sustainable Fibre  
168 Alliance, Grand Office, Ulaanbaatar, Mongolia. <sup>92</sup>The Dead-Sea and Arava Science Center,  
169 Yotvata, Israel. <sup>93</sup>Department of Geography and Earth Sciences. Aberystwyth University, Wales,  
170 UK. <sup>94</sup>School of Earth & Space Exploration, Arizona State University, Tempe, AZ, USA.  
171 <sup>95</sup>Science Division, Department of Planning, and Environment, New South Wales Government,  
172 Buronga, New South Wales, Australia. <sup>96</sup>ECOBIOISIS, Departement of Botany, University of  
173 Concepcion, Concepcion, Chile. <sup>97</sup>Zoology Department, National Museums of Kenya, Nairobi,  
174 Kenya. <sup>98</sup>Department of Earth and Environmental Sciences, Indiana University Indianapolis,  
175 Indianapolis, IN, USA. <sup>99</sup>Katif Research & Development Center, Sdot Negev, Netivot, Israel.  
176 <sup>100</sup>Kaye Academic College of Education, Beer Sheva, Israel. <sup>101</sup>State Key Laboratory of Desert  
177 and Oasis Ecology, Xinjiang Institute of Ecology and Geography, Chinese Academy of Sciences,  
178 Urumqi, China  
179  
180 email: [cesar.plaza@csic.es](mailto:cesar.plaza@csic.es); [eduardo.moreno@uam.es](mailto:eduardo.moreno@uam.es); [fernando.maestregil@kaust.edu.sa](mailto:fernando.maestregil@kaust.edu.sa)

181 **Mineral-associated organic carbon (MAOC) constitutes a major fraction of global soil**  
182 **carbon (C), and is assumed less sensitive to climate than particulate organic C (POC) due**  
183 **to protection by minerals. Despite its importance for long-term C storage, the response of**  
184 **MAOC to changing climates in drylands, which cover more than 40% of the global land**  
185 **area, remains unexplored. Here we assess topsoil organic C fractions across global**  
186 **drylands using a standardized field survey in 326 plots from 25 countries and six**  
187 **continents. We find that soil biogeochemistry explained the majority of variation in both**  
188 **MAOC and POC. Both C fractions decreased with increases in mean annual temperature**  
189 **and reductions in precipitation, with MAOC responding similarly to POC. Therefore, our**  
190 **results suggest that ongoing climate warming and aridification may result in unforeseen C**  
191 **losses across global drylands, and that the protective role of minerals may not dampen**  
192 **these effects.**

193  
194 Soils in drylands—the largest set of biomes of the planet —store 646 Pg of organic C, more than  
195 all living vegetation on Earth <sup>1,2</sup>. This vast soil organic C pool supports essential ecosystem  
196 services, including food provision and water and climate regulation for more than 2.5 billion  
197 people <sup>3,4</sup>. Yet, temperature increases and precipitation reductions forecasted for many dryland  
198 regions are expected to disrupt the balance of soil organic C, accelerating microbial  
199 decomposition, reducing plant C inputs into the soil, and resulting in more CO<sub>2</sub> emissions to the  
200 atmosphere <sup>5,6</sup>.

201 The sensitivity of organic C in soils (sensu ref. <sup>7</sup>) to temperature and precipitation at  
202 timescales relevant to climate change mitigation is thought to be controlled largely by  
203 interactions with soil minerals, which restrict the accessibility of microbial decomposers by

204 encapsulating and adsorbing organic matter<sup>8–10</sup>. Plant-derived materials at early stages of  
205 decomposition are the main constituents of the mineral-unprotected, particulate organic C (POC)  
206 fraction of soil organic matter<sup>9</sup>. The POC fraction is thus directly affected by changes in plant C  
207 inputs into the soil and is more exposed to microbial decomposition than the organic component  
208 of the mineral-associated organic C (MAOC) fraction, which has, therefore, a lower turnover rate  
209<sup>11,12</sup>. As a result, large scale meta-analyses and observational studies suggest that POC is more  
210 sensitive to changes in climate, and particularly to warming, than MAOC<sup>7,13–16</sup>. Because of the  
211 typically large ratio of soil minerals to organic matter in drylands, MAOC is expected to  
212 dominate over POC, potentially driving a high persistence of soil organic C in these ecosystems  
213<sup>7,10,17</sup>. However, no studies to date have examined the relationship of POC and MAOC with  
214 climate across the diverse environmental gradients that characterize global drylands.

215 Investigating this relationship is particularly timely and relevant, as it would significantly reduce  
216 the uncertainty surrounding the land carbon-climate feedback. Additionally, it would provide  
217 valuable insights for adapting soil carbon-related ecosystem services to ongoing climate change.

218 Here we evaluated how mean annual temperature and precipitation relates to POC and  
219 MAOC contents across global drylands after accounting for major biotic (net primary  
220 productivity, vegetation type, woody cover, plant and herbivore richness, and grazing pressure)  
221 and soil biogeochemistry (clay and silt contents, pH, chemical index of alteration, exchangeable  
222 Ca, non-crystalline Al and Fe, available N and P, and microbial biomass C) factors known to  
223 potentially affect soil organic C content by regulating C inputs and stabilization processes<sup>5,18</sup>. To  
224 do so, we surveyed *in situ* 326 plots from 98 dryland ecosystems located in 25 countries from six  
225 continents (Extended Data Fig. 1). Our survey spans the broad gradients of temperature,  
226 precipitation, aridity, soil properties, vegetation types, and grazing pressures that can be found

227 across drylands worldwide (Extended Data Tables 1 and 2)<sup>19,20</sup>. At each site, we collected  
228 topsoil samples (0-7.5 cm) from areas both covered (322) and not covered (326) by perennial  
229 vegetation from two to four plots located across a local gradient of extensive grazing pressure  
230 (648 samples in total, see Methods). We subjected all samples to a size fractionation procedure  
231 to separate and quantify C content in POC and MAOC pools<sup>9,21</sup>. Using these data, we tested the  
232 hypothesis that MAOC, being protected by minerals, is less sensitive than POC to increases in  
233 temperature and decreases in precipitation<sup>7,10,16,22</sup>. We also hypothesize that the presence of  
234 vegetation mitigates declines in soil C, particularly POC, by increasing soil C inputs.

235

### 236 **MAOC dominates soil organic C and is sensitive to climate**

237 Our results show that MAOC was the dominant soil organic C fraction in drylands globally (Fig.  
238 1a). In particular, median MAOC content was 5.2 g C kg<sup>-1</sup> soil, equivalent to 66% of the total  
239 soil organic C content, whereas median POC content was 2.3 g C kg<sup>-1</sup> soil. This quantification  
240 falls within the range of soil organic C content (MAOC and POC) commonly found in drylands,  
241 and is relevant to improve the performance of emerging models of soil organic C formation and  
242 persistence using POC and MAOC frameworks<sup>2, 23-25</sup>.

243 Contrary to our hypothesis, we found that MAOC and POC were equally sensitive to  
244 differences in climate across global drylands. In particular, both MAOC and POC were  
245 negatively associated with increasing temperature and decreasing precipitation to a similar  
246 extent, as indicated by the similar slopes of the associations (Fig. 1bc). These results were  
247 supported by the lack of a significant interaction between the effects of temperature and  
248 precipitation and the type of fraction (MAOC versus POC) tested by a linear mixed-effects  
249 model (Fig. 1d, see Methods). Based on the results from this model, we estimated that POC and



250 MAOC contents significantly declined with temperature at an average rate of 3.2% per °C (95%  
251 confidence interval (CI): 1.8, 4.6) and increased with precipitation at an average rate of 6.6% per  
252 100 mm (95% CI: 0.6, 12.6).

253 Warming accelerates the microbial decomposition of soil organic matter, and precipitation  
254 reduction constrains plant production and organic matter inputs into the soil <sup>5,26</sup>. Our results are,  
255 therefore, consistent with previously reported reductions in soil organic C content with  
256 increasing temperature and reducing precipitation across terrestrial ecosystems <sup>27-29</sup>. However,  
257 and contrary to expectations of smaller sensitivity of MAOC versus POC to changes in climate  
258 observed in more mesic systems <sup>14,15</sup>, our findings based on a space-for-time substitution  
259 highlight that the MAOC and POC fractions may decrease at similar rates in response to climate  
260 warming and precipitation reduction across global drylands. Therefore, they suggest that the  
261 current paradigm of mineral protection may not determine soil C persistence in dryland  
262 ecosystems <sup>8,30-32</sup>. The apparent lack of protection by minerals, which contrasts with what was  
263 observed in mesic systems richer in organic matter, was consistent across the range of soil  
264 organic C content found in drylands (Extended Data Fig. 2). There is recent evidence that  
265 MAOC is controlled not only by C stabilization in soil organo-mineral complexes, but also by  
266 changes in C inputs driven by climate <sup>15</sup>. In drylands, not only precipitation reduction but also  
267 warming may increase water deficit, which may decrease plant productivity <sup>5</sup>, C inputs into the  
268 soil and C accumulation into the MAOC fraction. These is also evidence that dryland soils  
269 maintain a high oxidative potential during dry periods, mainly through the stabilization of  
270 enzymes, which result in a rapid organic matter decomposition in wet periods <sup>28,29</sup> and may  
271 further limit C inputs to the MAOC fraction.

272

### 273 **Vegetation buffers soil C declines with warming**

274 Both POC and MAOC contents were higher in soil beneath perennial vegetation (Fig. 2). We  
275 further observed that as mean annual temperature increased, POC and MAOC contents  
276 decreased, but to a lesser extent, beneath vegetation. Conversely, as mean annual precipitation  
277 increased, both contents increased in a similar manner in open areas and in areas under the  
278 canopy of perennial vegetation (Fig. 2). These results are important because they suggest that the  
279 presence of vegetation buffers, but does not fully compensate for, the negative effects of higher  
280 temperature on soil C fractions. While the buffering effect of vegetation did not completely  
281 counteract the vulnerability of organic C pools to increasing temperatures, our findings indicate  
282 that management practices aimed at protecting vegetation in drylands may help to maintain soil  
283 organic C stocks in global drylands and reducing their losses in response to a changing climate.

284

### 285 **Coupling of POC and MAOC in drylands**

286 We found that POC and MAOC contents were strongly correlated across global drylands ( $r =$   
287  $0.83$ ,  $n = 326$ ,  $P < 0.001$ ; Fig. 3a). These results strongly suggest that both fractions remain  
288 highly coupled in drylands despite their different levels of putative protection against  
289 decomposition by microorganisms.

290 Variance partitioning of linear mixed-effects models and random forest analysis showed that  
291 the order of importance of the group of factors that explained most of the variation of POC and  
292 MAOC across global drylands was essentially the same for both organic C fractions (Fig. 3b,  
293 Extended Data Fig. 3). Soil biogeochemistry, above climate and biotic factors, was the most  
294 important predictor of both POC and MAOC contents. Both C fractions were negatively  
295 associated with soil pH and positively associated to exchangeable Ca, available N and P, and

296 microbial biomass C contents; additionally, MAOC was associated positively with clay and silt  
297 and non-crystalline Al and Fe contents (Extended Data Fig. 4). Slightly-acidic-to-neutral soils  
298 generally feature higher nutrient availability and more fertility than alkaline soils<sup>33</sup>, which may  
299 thus favor soil organic C accumulation in drylands through increased plant-derived C inputs and  
300 microbial activity. The prevalent role of soil fine texture and non-crystalline Al and Fe in MAOC  
301 formation has been widely documented in the literature<sup>31</sup>. Sorption of organic matter to mineral  
302 surfaces is known to be promoted by the relatively high specific surface area and charge of clay  
303 and silt, while non-crystalline Fe and Al phases are also known to form strong associations with  
304 organic matter<sup>31</sup>.

305 The coupling of POC and MAOC observed here for drylands may be, however, disrupted in  
306 more productive terrestrial ecosystems, where higher plant inputs may result in larger POC  
307 contents<sup>13–15</sup>. In contrast to experimental manipulation studies<sup>14</sup>, our work addresses the  
308 vulnerability of soil C fractions using a space-for-time substitution. Further research into the  
309 pace of the climate-induced changes and the causality of the associations found in our study is  
310 thus warranted.

311

## 312 **Concluding remarks**

313 By using a global standardized field study and by focusing exclusively on dryland ecosystems,  
314 our work expands previous efforts to understand abiotic and biotic drivers of POC and MAOC  
315 along large geographical gradients, which have either been based on literature syntheses, which  
316 use datasets that are inherently heterogenous, or have focused on ecosystems other than drylands  
317<sup>16</sup>. Our study generated highly standardized field data on the POC and MAOC fractions of

318 dryland soils worldwide, along with their major predictors. These data significantly expand  
319 existing global databases and can be used to refine current soil organic C models.

320 Our findings suggest that ongoing changes in climate, particularly warming, may adversely  
321 affect both unprotected and mineral-protected soil C content in drylands to a similar extent. The  
322 results obtained also indicate that maintaining vegetation cover can mitigate, but not fully  
323 counteract, the negative impacts of rising temperatures on soil organic C fractions. Our study  
324 enhances our understanding of how POC and MAOC contents in soil respond to key abiotic and  
325 biotic drivers, revealing that mineral protection has limited potential to sustain organic C storage  
326 in dryland soils in the face of ongoing global warming. The novel insights about dryland soil C  
327 pools and their sensitivity provided here could facilitate much-needed advances in our model  
328 representation of dryland ecosystems and their response to climate change.

329

330

### 331 **Acknowledgements**

332 This research was funded by the European Research Council (ERC Grant agreement 647038,  
333 BIODESERT), the Spanish Ministry of Science and Innovation (PID2020-116578RB-I00), and  
334 Generalitat Valenciana (CIDEGENT/2018/041), with additional support by the University of  
335 Alicante (UADIF22-74 and VIGROB22-350). F.T.M. acknowledges support from the King  
336 Abdullah University of Science and Technology (KAUST) and the KAUST Climate and  
337 Livability Initiative. D.J.E. is supported by the Hermon Slade Foundation. H.S. was supported by  
338 a María Zambrano fellowship funded by the Ministry of Universities and European Union-Next  
339 Generation plan. L.W. acknowledges support from the US National Science Foundation (EAR  
340 1554894). B.B. and S.S. were supported by the Taylor Family-Asia Foundation Endowed Chair

341 in Ecology and Conservation Biology. MB acknowledges support from a Ramón y Cajal grant  
342 from the Spanish Ministry of Science (RYC2021-031797-I). A.L. and L.K. acknowledge support  
343 from the German Research Foundation, DFG (grant CRC TRR228) and German Federal  
344 Government for Science and Education, BMBF (grants 01LL1802C and 01LC1821A). L.K.  
345 acknowledges travel funds from the Hans Merensky Foundation. A.N. and C.Br. acknowledge  
346 support from FCT - Fundação para a Ciência e a Tecnologia (CEECIND/02453/2018/CP1534/  
347 CT0001, PTDC/ASP-SIL/7743/ 2020, UIDB/00329/2020), from AdaptForGrazing project (PRR-  
348 C05-i03-I-000035) and from LTsER Montado platform (LTER\_EU\_PT\_001). S.C.R. was  
349 supported by NASA (NNH22OB92A) and is grateful to Erika Geiger, Armin Howell, Robin  
350 Reibold, Nick Melone, and Megan Starbuck for field support. Any use of trade, firm, or product  
351 names is for descriptive purposes only and does not imply endorsement by the U.S. Government.  
352 We thank the landowners for granting access to the sites and many people and their institutions  
353 for supporting our fieldwork activities: Louis Eloff, Dr Jorrie J. Jordaan, Dr Edwin Mudongo, Dr  
354 Vincent Mokoka, Baltimore Mokhou, Thabang Maphanga, Dr Dave Thompson (SAEON), Dr  
355 Anke S. K. Frank, Rose Matjea, Florian Hoffmann, Chris Goebel, the University of Limpopo,  
356 South African Environmental Observation Network (SAEON), the South African Military, and  
357 the Scientific Services Kruger National Park.

358

### 359 **Author contributions**

360 F.T.M. designed and coordinated the global field survey. C.P., F.T.M., and E.M.J. conceived this  
361 study. D.J.E., H.S., N.G., Y.L.B-P., B.G., V.O., E.G., M.G.G., E.V., S.A., M.B., J.M.V., B.J.M.,  
362 W.F., N.E., S.C., M.A., R.J.A., J.M.A., F.A., V.A, A.I.A., K.B., F.B.S., N.B., B.B., M.A.B.,  
363 D.B., C.Br., C.Bu., Y.C., R.Ca., A.P.C.M., I.C., P.C.Q., R.Ch., A.A.C., C.M.C., A.D.N., B.D.,

364 C.R.D., D.A.D., A.J.D., J.D., H.E., C.E., A.F., M.F., D.F., L.H., J.J.G., E.G.M., R.M.H.H.,  
365 A.v.H., N.H., E.H.S., F.M.H., O.J.M., F.J., A.J., M.J., K.F.K., L.K., J.E.L., P.C.L.R., P.L., A.L.,  
366 J.L., M.A.L., G.M.K., T.P.M., O.M.I., E.M., P.M., A.J.M., M.P.M., J.V.S.M., J.P.M., G.M.,  
367 S.M.M., A.N., G.O., G.R.O., B.O., G.P., Y.P., R.E.Q., S.C.R., V.M.R., A.Ro., J.C.R., O.S., A.S.,  
368 J.S., M.S., S.S., I.S., C.R.A.S., A.L.T., A.D.T., H.L.T., K.T., S.T., J.V., O.V., L.V.D.B., F.V.,  
369 W.W., D.W., L.W., G.M.W., L.Y., E.Z., J.M.Z., Y.Z., and X.Z. performed field research.  
370 P.D.M., V.O., B.G., B.J.M., S.C., N.E., J.C.G.G., C.Z., M.P., W.F., I.B.F., A.Re., E.M.J., and  
371 C.P. conducted laboratory research and analysis. P.D.M., E.G., and C.P. carried out data  
372 analysis, after discussion, suggestions, and contributions from F.T.M., E.M.J., M.D.B., N.G.,  
373 Y.L.B-P., H.S., C.Z., M.P., P.G.P., A.Re., M.B., and S.M.M. P.D.M. and C.P. wrote the original  
374 manuscript draft, with contributions from F.T.M., E.M.J., and M.D.B. All authors discussed the  
375 results and contributed to editing the manuscript.

376

### 377 **Competing interests**

378 The authors declare no competing interests.

379

### 380 **Figure captions**

381

382 **Fig. 1 | Distribution of soil organic carbon (C) contents in particulate organic C (POC) and**  
383 **mineral-associated organic C (MAOC) fractions and their relationships with climate in**  
384 **global drylands. a**, Boxplot of POC and MAOC contents. Box, 1<sup>st</sup>, and 3<sup>rd</sup> quartiles; central  
385 horizontal line, median; upper vertical line end, largest value smaller than 1.5 times the  
386 interquartile range; lower vertical line, smallest value larger than 1.5 times the interquartile range  
387 ( $n = 326$  plots). **b-c**, Relationships between POC and MAOC contents and mean annual  
388 temperature (MAT, **b**) and precipitation (MAP, **c**). Lines and shading represent linear regressions  
389 and 95% confidence intervals. **d**, Summary of a linear mixed-effects model, controlling for biotic

390 factors and soil biogeochemistry (see Methods). The panel shows coefficients (circles) and 95%  
391 confidence intervals (CI, bars) for main and interaction effects of C fraction type (binary  
392 variable, either POC or MAOC) and climate (MAT and MAP) on POC and MAOC contents.  
393 The variance explained ( $R^2$ ) by the fixed and random effects relative to the total variance was  
394 77% and 12%, respectively ( $n = 634$  POC and MAOC observations). Carbon fraction contents  
395 were natural-logarithm transformed, and all the predictors were standardized. The positive  
396 coefficient of C fraction type (MAOC vs. POC) indicate that MAOC contents are significantly  
397 greater than POC contents ( $P < 0.001$ ). For the observed negative association of MAT and  
398 positive association of MAP with C content ( $P < 0.001$  and  $P = 0.039$  respectively), negative  
399 coefficients for the interaction of C fraction type with MAT and MAP indicate that increasing  
400 MAT has a stronger negative effect on MAOC than on POC contents ( $P = 0.053$ ), while  
401 decreasing MAP has a stronger negative effect on POC than on MAOC ( $P = 0.181$ ).

402 **Fig. 2 | Relationships between climate and particulate organic C (POC) and mineral-**  
403 **associated organic C (MAOC) contents in soils under the canopy of the dominant perennial**  
404 **vegetation (V) and in open areas (O) across global drylands. a-d**, Relationships between POC  
405 and mean annual temperature (MAT, **a**) and precipitation (MAP, **c**), and between MAOC and  
406 MAT (**b**) and MAP (**d**) in both O and V microsites. Lines and shading represent linear  
407 regressions and 95% confidence intervals ( $n = 326$  and  $322$  for O and V, respectively). **e**,  
408 Coefficients (dots) and 95% confidence intervals (bars) of linear mixed-effects model illustrating  
409 the fixed main and interaction effects of MAT, MAP, and the presence of vegetation cover (V vs.  
410 O) on POC and MAOC contents ( $n = 648$  V and O areas). The variance explained ( $R^2$ ) by the  
411 fixed and random effects relative to the total variance was 30% and 55%, respectively, for POC,  
412 and 32% and 61%, respectively, for MAOC.

413 **Fig. 3 | Coupling and drivers of particulate organic C (POC) and mineral-associated**  
414 **organic C (MAOC) in global drylands. a**, Relationship between POC and MAOC contents.  
415 Dots represent individual dryland plots, with the colors of the dots illustrating their aridity (1 –  
416 annual precipitation/potential evapotranspiration) values. The line and shading represent the  
417 fitted linear regression and 95% confidence interval, respectively. **b**, Variance explained ( $R^2$ ) by  
418 linear mixed-effects models for POC and MAOC contents partitioned into the fraction  
419 attributable to unique and shared among groups of drivers (climate: mean annual temperature  
420 and mean annual precipitation; biotic factors: net primary productivity, type of vegetation,

421 woody cover, plant richness, grazing pressure, and herbivore richness; and soil biogeochemistry:  
422 clay and silt, pH, chemical index of alteration, exchangeable Ca, non-crystalline Al and Fe,  
423 available N and P, and microbial biomass carbon). The variance explained ( $R^2$ ) by the fixed and  
424 random effects relative to the total variance was 69% and 20% for POC ( $n = 317$ ) and 84% and  
425 11% for MAOC ( $n = 317$ ), respectively.

426

## 427 **References**

428

- 429 1. IPCC. Global Carbon and Other Biogeochemical Cycles and Feedbacks. in *Climate Change*  
430 *2021 – The Physical Science Basis* 673–816 (Cambridge University Press, 2023).
- 431 2. Plaza, C. et al. Soil resources and element stocks in drylands to face global issues. *Sci Rep* 8,  
432 (2018).
- 433 3. Maestre, F. T. et al. Structure and functioning of dryland ecosystems in a changing world.  
434 *Annu Rev Ecol Evol Syst* 47, 215–237 (2016).
- 435 4. Smith, P. et al. Biogeochemical cycles and biodiversity as key drivers of ecosystem services  
436 provided by soils. *SOIL* 1, 665–685 (2015).
- 437 5. Gaitán, J. J. et al. Biotic and abiotic drivers of topsoil organic carbon concentration in  
438 drylands have similar effects at regional and global scales. *Ecosystems* 22, 1445–1456  
439 (2019).
- 440 6. Huang, J., Yu, H., Guan, X., Wang, G. & Guo, R. Accelerated dryland expansion under  
441 climate change. *Nat Clim Chang* 6, 166–171 (2016).
- 442 7. Lugato, E., Lavallee, J. M., Haddix, M. L., Panagos, P. & Cotrufo, M. F. Different climate  
443 sensitivity of particulate and mineral-associated soil organic matter. *Nat Geosci* 14, 295–300  
444 (2021).
- 445 8. Hemingway, J. D. et al. Mineral protection regulates long-term global preservation of natural  
446 organic carbon. *Nature* 570, 228–231 (2019).
- 447 9. Lavallee, J. M., Soong, J. L. & Cotrufo, M. F. Conceptualizing soil organic matter into  
448 particulate and mineral-associated forms to address global change in the 21st century. *Glob*  
449 *Chang Biol* 26, 261–273 (2020).



- 450 10. Cotrufo, M. F. & Lavalley, J. M. Soil organic matter formation, persistence, and functioning:  
451 A synthesis of current understanding to inform its conservation and regeneration. in  
452 *Advances in Agronomy* (ed. Sparks, D. L.) vol. 172 1–66 (Academic Press, 2022).
- 453 11. Prairie, A. M., King, A. E. & Cotrufo, M. F. Restoring particulate and mineral-associated  
454 organic carbon through regenerative agriculture. *Proceedings of the National Academy of*  
455 *Sciences* 120, e2217481120 (2023).
- 456 12. Haddix, M. L., Paul, E. A. & Cotrufo, M. F. Dual, differential isotope labeling shows the  
457 preferential movement of labile plant constituents into mineral-bonded soil organic matter.  
458 *Glob Chang Biol* 22, 2301–2312 (2016).
- 459 13. Cotrufo, M. F., Ranalli, M. G., Haddix, M. L., Six, J. & Lugato, E. Soil carbon storage  
460 informed by particulate and mineral-associated organic matter. *Nat Geosci* 12, 989–994  
461 (2019).
- 462 14. Rocci, K. S., Lavalley, J. M., Stewart, C. E. & Cotrufo, M. F. Soil organic carbon response to  
463 global environmental change depends on its distribution between mineral-associated and  
464 particulate organic matter: A meta-analysis. *Sci Total Environ* 793, 148569 (2021).
- 465 15. Hansen, P. M. et al. Distinct, direct and climate-mediated environmental controls on global  
466 particulate and mineral-associated organic carbon storage. *Glob Chang Biol* 30, e17080  
467 (2024).
- 468 16. Georgiou, K. et al. Emergent temperature sensitivity of soil organic carbon driven by mineral  
469 associations. *Nat Geosci* 17, 205–212 (2024).
- 470 17. Cotrufo, F. M. et al. In-N-Out: A hierarchical framework to understand and predict soil  
471 carbon storage and nitrogen recycling. *Glob Chang Biol* 27, 4465–4468 (2021).
- 472 18. von Fromm, S. F. et al. Continental-scale controls on soil organic carbon across sub-Saharan  
473 Africa. *SOIL* 7, 305–332 (2021).
- 474 19. Maestre, F. T. et al. The BIODESERT survey: assessing the impacts of grazing on the  
475 structure and functioning of global drylands. *Web Ecol* 22, 75–96 (2022).
- 476 20. Maestre, F. T. et al. Grazing and ecosystem service delivery in global drylands. *Science*  
477 (1979) 378, 915–920 (2022).
- 478 21. Cambardella, C. A. & Elliot, E. T. Particulate soil organic-matter changes across a grassland  
479 cultivation sequence. *Soil Science Society of America Journal* 56, 777–783 (1992).

- 480 22. Cotrufo, M. F. et al. Formation of soil organic matter via biochemical and physical pathways  
481 of litter mass loss. *Nat Geosci* 8, 776–779 (2015).
- 482 23. Sokol, N. W. et al. Global distribution, formation and fate of mineral-associated soil organic  
483 matter under a changing climate: A trait-based perspective. *Funct Ecol* 36, 1411–1429  
484 (2022).
- 485 24. Wieder, W. R. et al. Carbon cycle confidence and uncertainty: Exploring variation among  
486 soil biogeochemical models. *Glob Chang Biol* 24, 1563–1579 (2018).
- 487 25. Sulman, B. N. et al. Multiple models and experiments underscore large uncertainty in soil  
488 carbon dynamics. *Biogeochemistry* 141, 109–123 (2018).
- 489 26. Davidson, E. A. & Janssens, I. A. Temperature sensitivity of soil carbon decomposition and  
490 feedbacks to climate change. *Nature* 440, 165–173 (2006).
- 491 27. Smith, K. R. & Waring, B. G. Broad-scale patterns of soil carbon (C) pools and fluxes across  
492 semiarid ecosystems are linked to climate and soil texture. *Ecosystems* 22, 742–753 (2018).
- 493 28. Darrouzet-Nardi, A. et al. Consistent microbial and nutrient resource island patterns during  
494 monsoon rain in a Chihuahuan Desert bajada shrubland. *Ecosphere* 14, e4475 (2023).
- 495 29. Stursova, M. & Sinsabaugh, R. L. Stabilization of oxidative enzymes in desert soil may limit  
496 organic matter accumulation. *Soil Biol Biochem* 40, 550–553 (2008).
- 497 30. Lehmann, J. & Kleber, M. The contentious nature of soil organic matter. *Nature* 528, 60–68  
498 (2015).
- 499 31. Kleber, M. et al. Mineral–Organic Associations: Formation, Properties, and Relevance in  
500 Soil Environments. in *Advances in Agronomy* (ed. Sparks, D. L.) vol. 130 1–140 (Academic  
501 Press, Waltham, MA, 2015).
- 502 32. Kleber, M. et al. Dynamic interactions at the mineral–organic matter interface. *Nat Rev Earth*  
503 *Environ* 2, 402–421 (2021).
- 504 33. Bardgett, R. D. *The Biology of Soil: A Community and Ecosystem Approach*. (Oxford  
505 University Press, United Kingdom, 2005).

506 **Methods**

507 **Global field survey and soil sampling.** Fieldwork was conducted from January 2016 to  
508 September 2019. A total of 326 plots distributed across 98 study sites in 25 countries from all  
509 continents except Antarctica (Algeria, Argentina, Australia, Botswana, Brazil, Canada, Chile,  
510 China, Ecuador, Hungary, Iran, Israel, Kazakhstan, Kenya, Mexico, Mongolia, Namibia, Niger,  
511 Palestine, Peru, Portugal, South Africa, Spain, Tunisia, and United States of America) and  
512 encompassing the wide range of vegetation, soil, climate, and grazing pressure levels found in  
513 drylands worldwide were surveyed using a common and standardized protocol <sup>19,20</sup>.

514 At each site, we gathered field data within multiple 45 m x 45 m plots situated along a  
515 gradient of grazing pressure, encompassing high (n = 98), medium (n = 97), and low (n = 88)  
516 pressure levels, as well as ungrazed areas (n = 43). To establish the grazing gradients, in 90 out  
517 of the 98 sites surveyed, we strategically positioned these plots at varying distances from  
518 artificial watering points, which are usually created in drylands to supply introduced livestock  
519 with permanent water sources <sup>34</sup>. The closer the plot to the permanent water source, the more  
520 intense the grazing <sup>34,35</sup>. In the remaining eight sites, local variations in grazing pressure  
521 gradients were ascertained by observing different paddocks featuring varying grazing intensities.  
522 See ref. <sup>20</sup> for additional details on the characterization and validation of the local grazing  
523 pressure gradients established.

524 A portable Global Positioning System was used to record the coordinates and elevation of  
525 each plot, which were standardized to the WGS84 ellipsoid for visualization and analyses.  
526 During the dry season at each site, four soil cores (145 cm<sup>3</sup>) from 0 to 7.5-cm depth (topsoil)  
527 were collected from five 50 × 50-cm quadrats randomly placed in areas under the canopy of the  
528 dominant perennial vegetation and five placed in open areas not covered by perennial vegetation.

529 The soil cores were homogenized and composited to form a sample representative of the soil  
530 under the dominant vegetation and a sample representative of the soil in open areas within each  
531 plot. The soil samples were passed through a 2-mm sieve. A portion of each soil sample was air-  
532 dried and used for organic matter fractionation and texture and pH analysis, and another portion  
533 was stored at -20 °C and used for microbial biomass C analysis. A portion of the air-dried soil  
534 samples was ground with a ball mill for additional chemical analysis.

535 **Soil organic carbon fractionation and quantification.** All the soil samples, a total of 648 (326  
536 from open areas and 322 from under the canopy of the dominant vegetation), were subjected to a  
537 size fractionation method <sup>21,36</sup> to separate the POC (not protected by minerals from microbial  
538 decomposition) and MAOC (protected by minerals) fractions. Aggregates were dispersed by  
539 adding 30 mL of sodium hexametaphosphate (5 g L<sup>-1</sup>) to 10 g of soil and shaking with an  
540 overhead shaker for 18 h. After dispersion, the mixture was thoroughly rinsed through a 53- $\mu$ m  
541 sieve, to separate the POC (> 53  $\mu$ m) and MAOC (< 53  $\mu$ m) fractions using an automated wet  
542 sieving system. The isolated fractions were oven-dried at 60 °C, weighed, and ground with a ball  
543 mill. The whole soil samples and the POC and MAOC fractions were analyzed for organic C  
544 contents by dry combustion and gas chromatography using a ThermoFlash 2000 NC Soil  
545 Analyzer (Thermo Fisher Scientific, MA) after removing carbonates by acid fumigation <sup>37</sup>.

546 **Climate data.** Mean annual temperature and mean annual precipitation data were obtained from  
547 WorldClim 2.0 <sup>38</sup> a high resolution (30 arc seconds or ~ 1 km at the equator) database based on a  
548 large number of climate observations and topographical data for the 1970-2000 period. Aridity  
549 index (ratio of average annual precipitation to potential evapotranspiration) data were obtained  
550 from the Global Aridity Index and Potential Evapotranspiration Climate Database v3 <sup>39</sup>. Aridity  
551 was calculated as 1 – aridity index.

552 **Vegetation and herbivore richness survey.** Each plot was classified as grassland, shrubland, or  
553 forest by identifying the dominant type of vegetation. Net primary productivity (NPP) was  
554 estimated using the mean annual Normalized Difference Vegetation Index (NDVI) averaged  
555 monthly values between 1999 and 2019 at a resolution of 30 m from Landsat 7 Enhanced  
556 Thematic Mapper Plus (ETM+) <sup>40</sup>. The cover of perennial vascular plants (plant cover) was  
557 measured along four parallel 45-m transects separated by 10 m and oriented downslope during  
558 the peak of the growing season using the line-intercept method <sup>19,41,42</sup>. Woody cover was  
559 measured in 25 contiguous quadrats (1.5 m × 1.5 m) placed in each transect (100 quadrats per  
560 plot). Plant richness was the total number of unique perennial species found along the quadrats  
561 and transects surveyed. The richness of herbivores was quantified at each plot using dung data  
562 collected systematically in situ along the four 45-m transects established as described in ref. <sup>20</sup>.

563 **Soil analyses.** All the bulk soil samples were analyzed as follows. Clay and silt contents were  
564 determined by sieving and sedimentation <sup>43</sup>. Soil pH was measured in a water suspension at a  
565 soil-to-water ratio of 1:2.5 <sup>44</sup>. The chemical index of alteration, which is an indicator of the  
566 degree of weathering, was calculated as the molecular proportion of Al<sub>2</sub>O<sub>3</sub> versus Al<sub>2</sub>O<sub>3</sub> + CaO +  
567 Na<sub>2</sub>O + K<sub>2</sub>O <sup>45</sup>, using total Al, Ca, Na, and K contents and after correcting Ca for soils with  
568 carbonates <sup>18</sup>; total Al, Ca, Na and K contents were determined by inductively coupled plasma  
569 atomic emission spectroscopy (ICP-AES) after digestion in nitric and perchloric acids <sup>44,46</sup>.

570 Exchangeable Ca content was determined by ICP-AES after extraction with ammonium acetate  
571 at pH 7.0 <sup>44,47</sup>. Non-crystalline Fe and Al contents were determined by ICP-AES after extraction  
572 with acid ammonium oxalate <sup>48</sup>. Available N (ammonium and nitrate) content was determined by  
573 extraction with 0.5 M K<sub>2</sub>SO<sub>4</sub> and the indophenol blue method using a microplate reader <sup>49</sup>.

574 Available P content was determined by the Olsen method <sup>50</sup>. Microbial biomass C was  
575 determined by substrate-induced respiration <sup>51</sup> using an automated microrespirometer <sup>52</sup>.

576 **Statistical analyses.** We compared the content of MAOC with that of POC in global dryland  
577 soils controlling for confounding factors, and tested the hypothesis that the effects of climate  
578 (mean annual temperature and precipitation) on POC and MAOC contents depends on (interacts  
579 with) the C fraction type. For these analyses, we aggregated soil data for open and vegetation  
580 covered areas by plot using plant cover area as a weighting factor, and fitted a linear mixed-  
581 effects model on the response of C content with C fraction type as a binary categorical predictor  
582 (either MAOC or POC). In the fixed-effects term of the model, we also included mean annual  
583 temperature, mean annual precipitation, and the interactions of mean annual temperature and  
584 mean annual precipitation with C fraction type, as well as key biotic (net primary productivity,  
585 type of vegetation, woody cover, plant richness, grazing pressure, and herbivore richness) and  
586 soil biogeochemical (clay and silt, pH, chemical index of alteration, exchangeable Ca, non-  
587 crystalline Al and Fe, available N and P, and microbial biomass C) covariates to control for  
588 confounding factors. In the random term of the model, we incorporated an intercept structure  
589 with plot nested within site as a categorical variable to account for the lack of independence in  
590 the residuals due to the paired POC and MAOC separation and the plot sampling design. We  
591 checked whether the fit of this linear mixed-effects model improved by including quadratic terms  
592 of mean annual temperature, mean annual precipitation, and both mean annual temperature and  
593 precipitation, using the Akaike information criterion (AIC) and likelihood ratio tests. None of the  
594 quadratic models tested was a significantly better fit to the data ( $\chi^2 (1) < 1.0$ ,  $P > 0.3$ ) than the  
595 linear model (lowest AIC).

596 To examine separately the variance of POC and MAOC contents explained by the groups of  
597 predictors (climate: mean annual temperature and mean annual precipitation; biotic factors: net  
598 primary productivity, type of vegetation, woody cover, plant richness, grazing pressure, and  
599 herbivore richness; soil biogeochemistry: clay and silt, pH, chemical index of alteration,  
600 exchangeable Ca, non-crystalline Al and Fe, available N and P, and microbial biomass C), we  
601 built two linear mixed-effects models (one for POC and another one for MAOC) with site as a  
602 random categorical variable. These two separate models were used to assess the importance of  
603 the different groups of predictors in explaining either POC or MAOC, and not to test statistically  
604 for differences in the size of the effects of the predictors between POC and MAOC. To support  
605 the linear mixed-effects models, we tested the importance of the same groups of predictors of  
606 POC and MAOC using random forest regression modeling<sup>53</sup>. In particular, we built two random  
607 forest models, one for POC and one for MAOC, combining 500 trees, and quantified the  
608 importance of each predictor by computing the increase in mean squared error across trees when  
609 the predictor was permuted.

610 We tested whether the presence of vegetation cover interacted with the effects of temperature  
611 and precipitation also by linear mixed-effects modeling. For this purpose, we built two linear  
612 mixed-effects models, one for POC content and another one for MAOC content in areas under  
613 the canopy of the dominant perennial vegetation and open areas, with vegetation cover as a  
614 binary predictor and plot nested within site in the random term.

615 For all the linear mixed-effects models, POC, MAOC, exchangeable Ca, non-crystalline Al  
616 and Fe, available N and P, and microbial biomass C were natural-logarithm transformed to  
617 reduce the skewness of the data. To compare effect sizes, all the numeric predictors were  
618 standardized by subtracting the mean and dividing by two standard deviations, and the binary

619 variables (C fraction type and vegetated vs. open areas) were rescaled to -0.5 and 0.5 <sup>54</sup>. The  
620 coefficients of the models were estimated by the restricted maximum likelihood approach, 95%  
621 confidence intervals were calculated, and P-values were computed based on Satterthwaite  
622 approximation <sup>55</sup>. The validity of the assumptions of normality, homoscedasticity and linearity  
623 were examined using residual plots. The generalized variance inflation factors (GVIFs) were  
624 computed to check for multicollinearity among predictors (GVIF values were less than 3 in all  
625 cases, suggesting that multicollinearity was low <sup>56</sup>). All statistical analyses were performed using  
626 R <sup>57</sup> and the R packages arm <sup>58</sup>, ggplot2 <sup>59</sup>, lme4 <sup>60</sup>, lmerTest <sup>55</sup>, partR2 <sup>61</sup>, patchwork <sup>62</sup>,  
627 rnatualearth <sup>63</sup>, randomForest <sup>64</sup>, sf <sup>65</sup>, terra <sup>66</sup>, and viridis <sup>67</sup>.

628

## 629 **Data availability**

630 The data associated with this study are publicly available in

631 <https://figshare.com/s/8aeac2300650181f2c86> (<https://doi.org/10.6084/m9.figshare.24678891>) <sup>68</sup>.

632

## 633 **Methods-only references**

634 34. Fensham, R. J. & Fairfax, R. J. Water-remoteness for grazing relief in Australian arid-lands.  
635 Biol Conserv 141, 1447–1460 (2008).

636 35. Fensham, R. J., Fairfax, R. J. & Dwyer, J. M. Vegetation responses to the first 20 years of  
637 cattle grazing in an Australian desert. Ecology 91, 681–692 (2010).

638 36. Sokol, N. W. & Bradford, M. A. Microbial formation of stable soil carbon is more efficient  
639 from belowground than aboveground input. Nat Geosci 12, 46–53 (2019).

640 37. Harris, D., Horwath, W. R. & Van Kessel, C. Acid fumigation of soils to remove carbonates  
641 prior to total organic carbon or carbon-13 isotopic analysis. Soil Sci Soc Am J 65, 1853–  
642 1856 (2001).

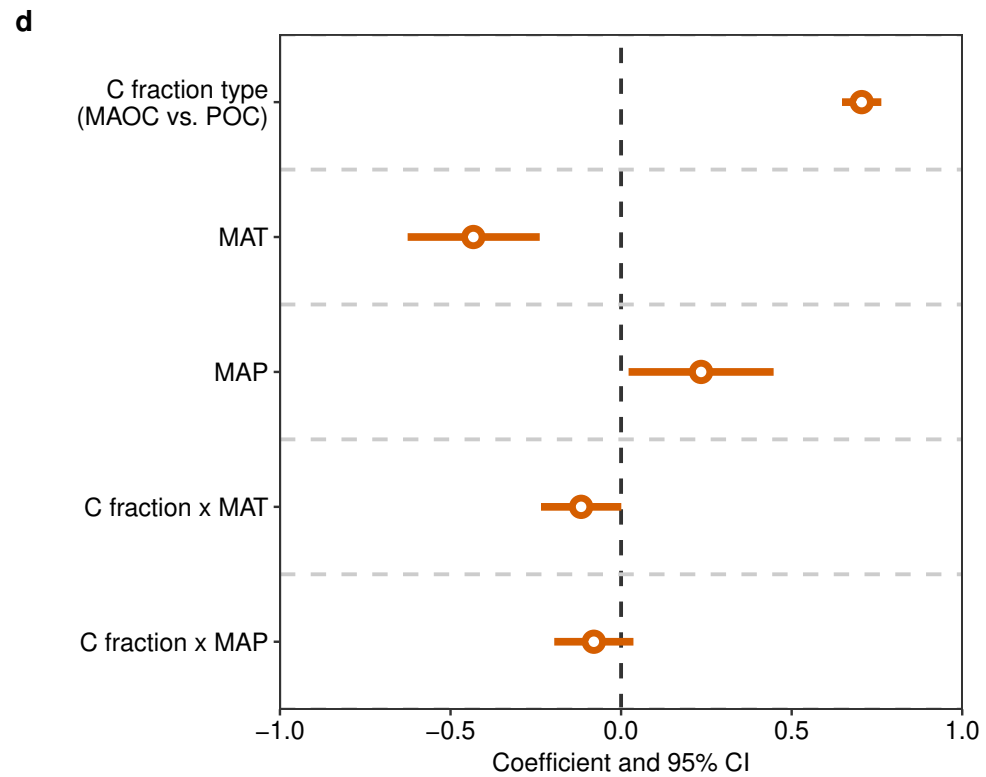
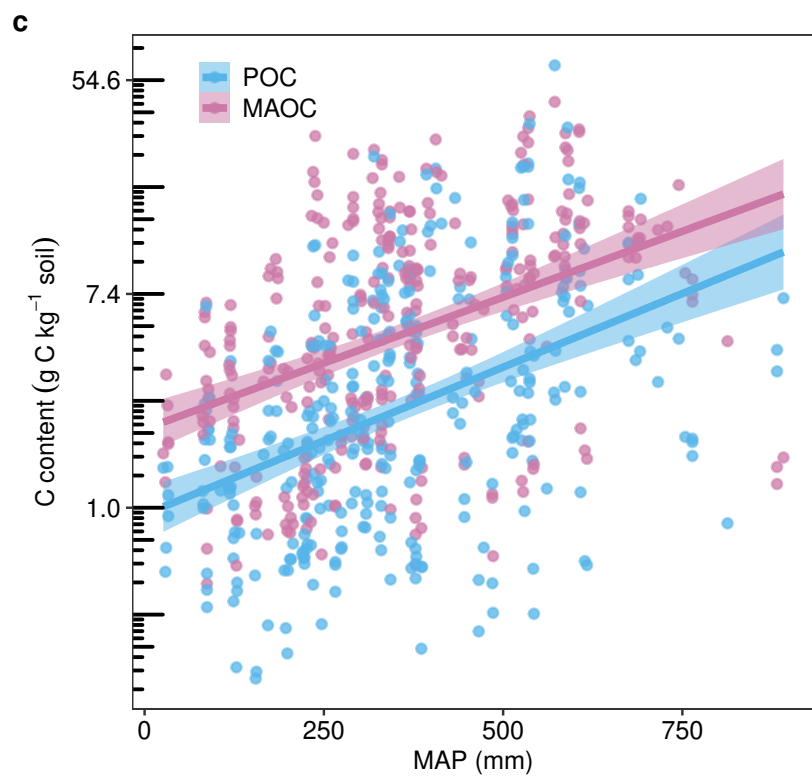
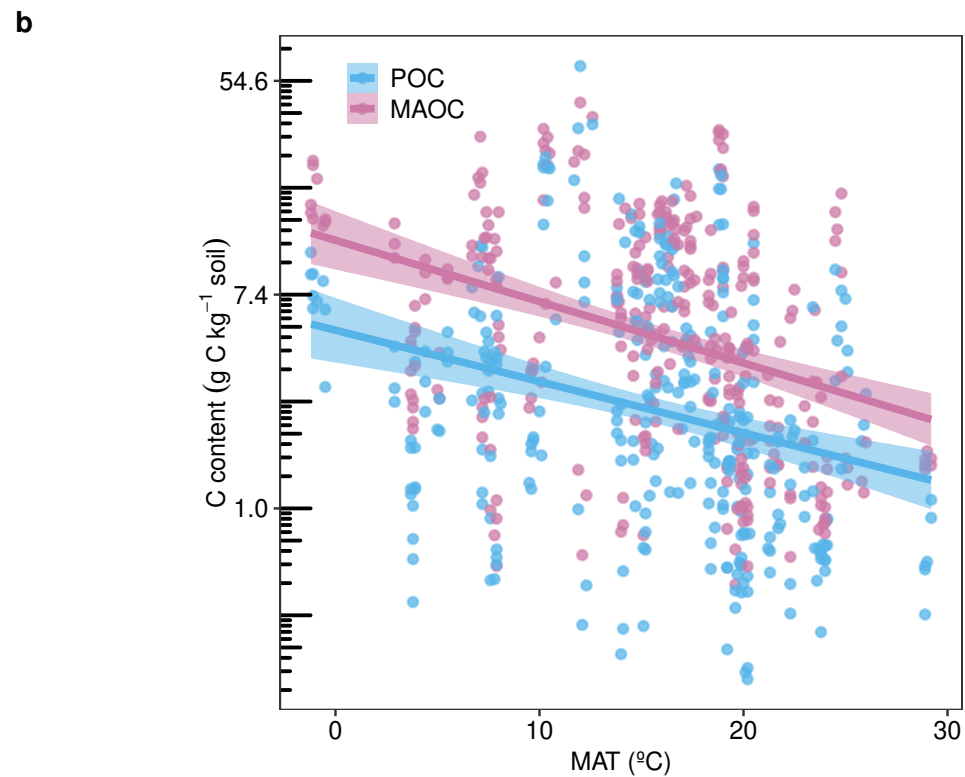
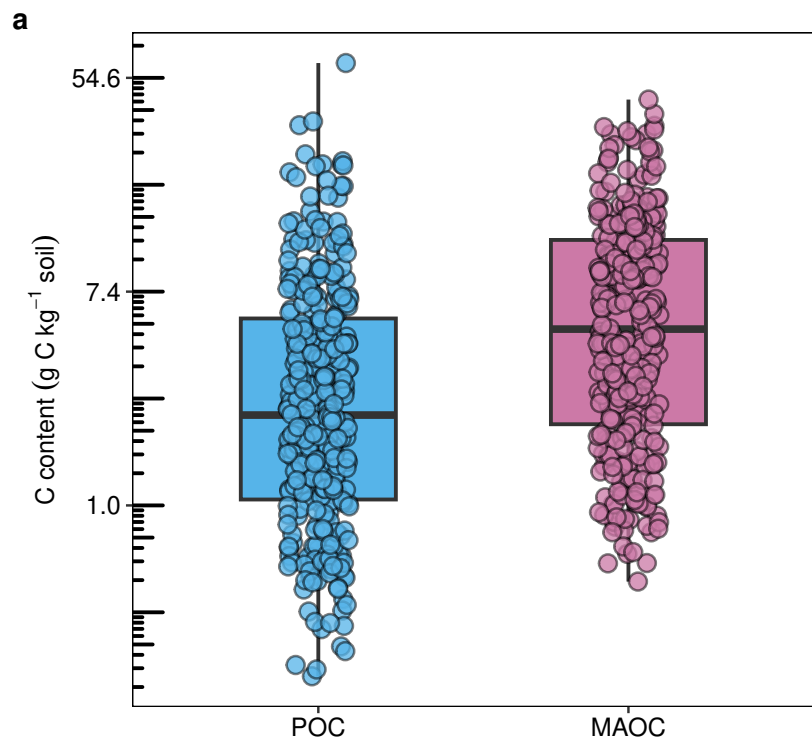
643 38. Fick, S. E. & Hijmans, R. J. WorldClim 2: new 1-km spatial resolution climate surfaces for  
644 global land areas. Int J Climatol 37, 4302–4315 (2017).

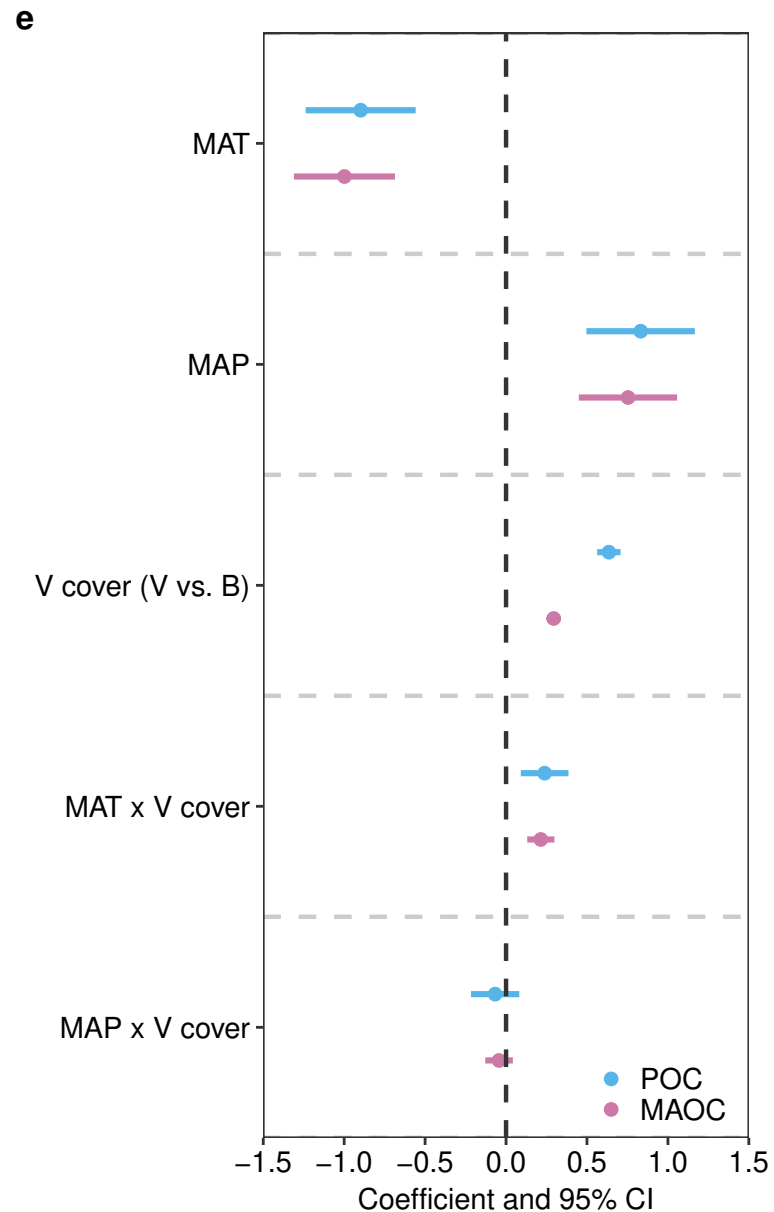
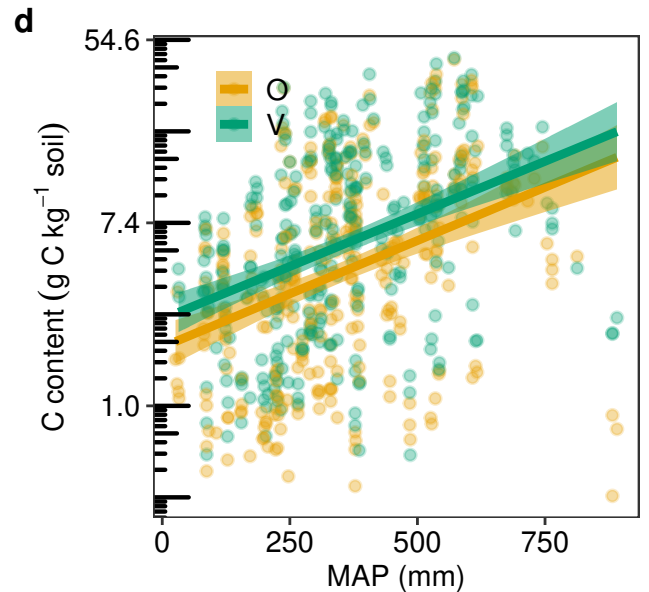
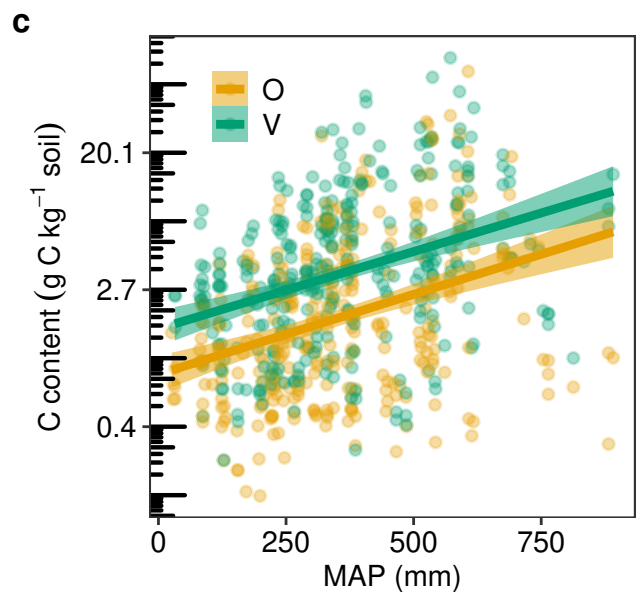
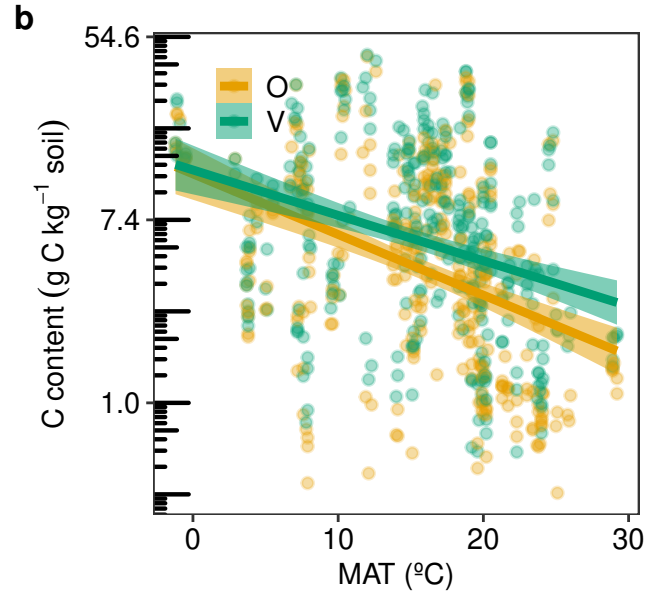
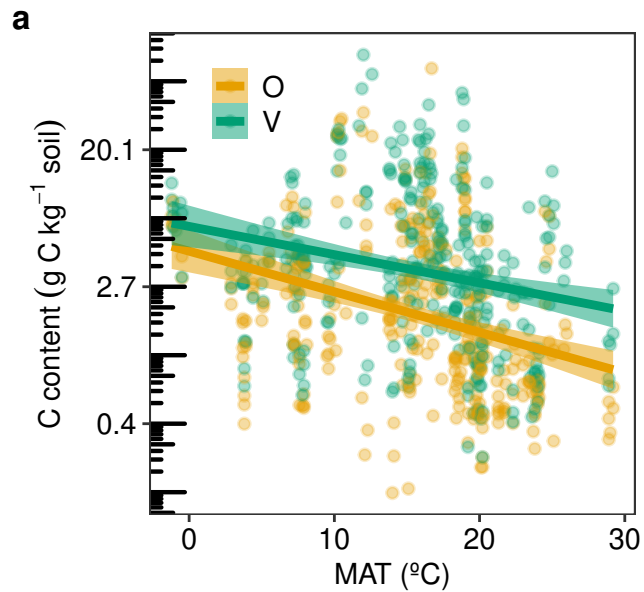


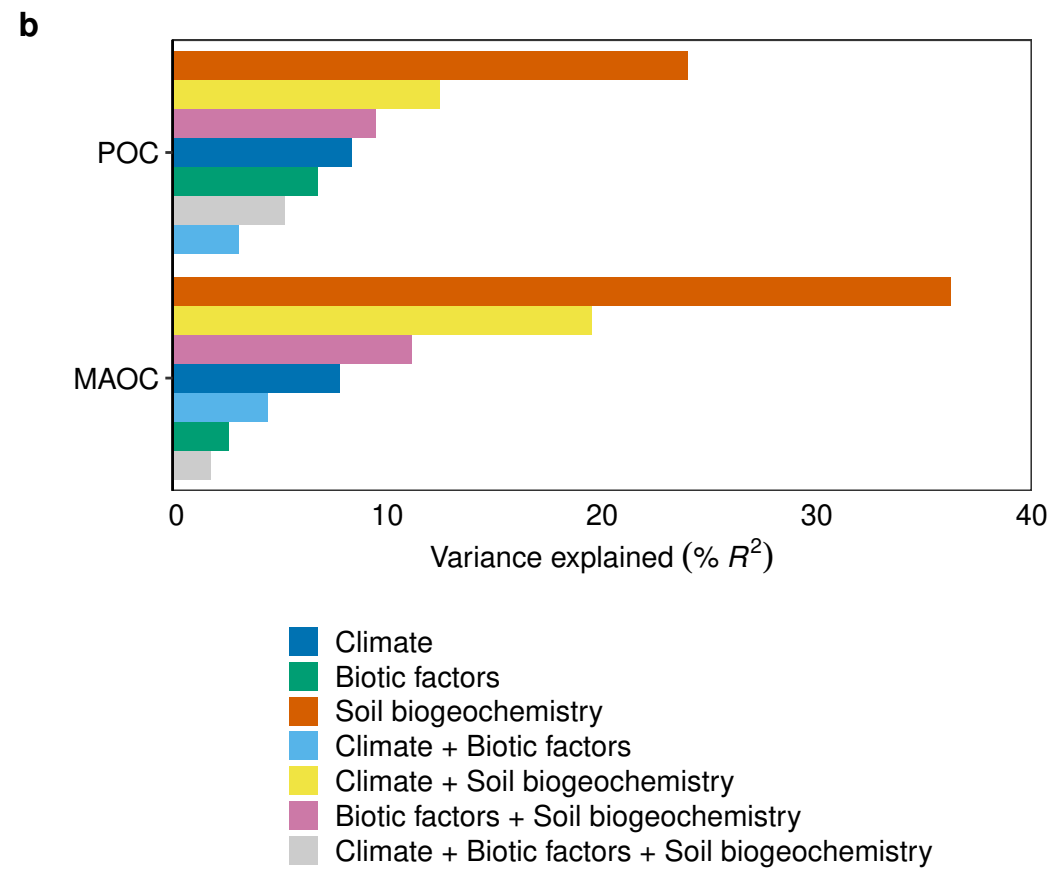
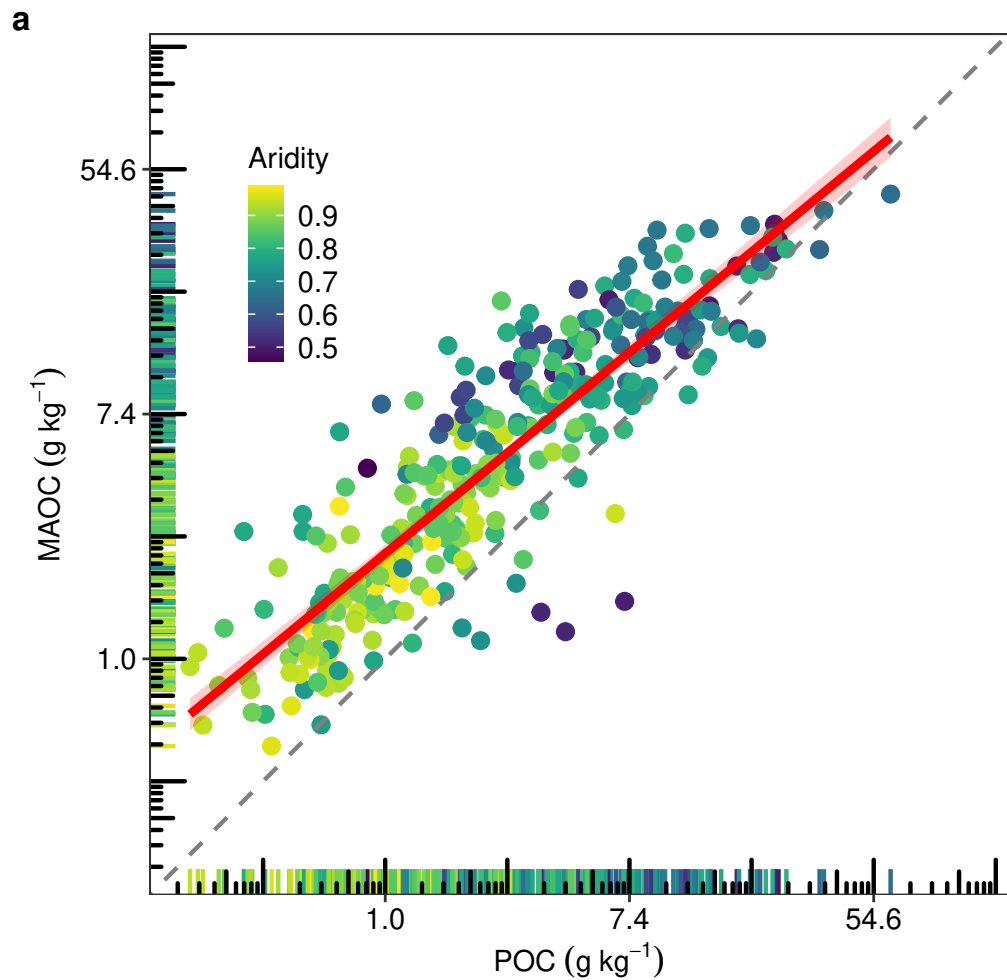
- 645 39. Zomer, R. J., Xu, J. & Trabucco, A. Version 3 of the Global Aridity Index and Potential  
646 Evapotranspiration Database. *Sci Data* 9, 409 (2022).
- 647 40. Vermote, E., Justice, C., Claverie, M. & Franch, B. Preliminary analysis of the performance  
648 of the Landsat 8/OLI land surface reflectance product. *Remote Sens Environ* 185, 46–56  
649 (2016).
- 650 41. Levi, E. B. & Madden, E. A. The point method of pasture analysis. *New Zealand J. Agric.*  
651 46, 267–279 (1933).
- 652 42. Maestre, F. T. et al. Plant species richness and ecosystem multifunctionality in global  
653 drylands. *Science* (1979) 335, 214–218 (2012).
- 654 43. Kettler, T. A., Doran, J. W. & Gilbert, T. L. Simplified method for soil particle-size  
655 determination to accompany soil-quality analyses. *Soil Sci Soc Am J* 65, 849–852 (2001).
- 656 44. Sparks, D. L. et al. *Methods of Soil Analyses, Part 3: Chemical Methods.* (Soil Science  
657 Society of America, American Society of Agronomy, 1996).
- 658 45. Nesbitt, H. W. & Young, G. M. Early proterozoic climates and plate motions inferred from  
659 major element chemistry of lutites. *Nature* 299, 715–717 (1982).
- 660 46. Hesse, P. R. *A Textbook of Soil Chemical Analysis.* (John Murray, London, 1971).
- 661 47. Rasmussen, C. et al. Beyond clay: towards an improved set of variables for predicting soil  
662 organic matter content. *Biogeochemistry* 137, 297–306 (2018).
- 663 48. Darke, A. K. & Walbridge, M. R. Estimating non-crystalline and crystalline aluminum and  
664 iron by selective dissolution in a riparian forest soil. *Commun Soil Sci Plant Anal* 25, 2089–  
665 2101 (1994).
- 666 49. Sims, G. K., Ellsworth, T. R. & Mulvaney, R. L. Microscale determination of inorganic  
667 nitrogen in water and soil extracts. *Commun Soil Sci Plant Anal* 26, 303–316 (1995).
- 668 50. Olsen, S. R. & Sommers, L. E. Phosphorus. in *Methods of Soil Analysis. Part 2. Chemical*  
669 *and Microbiological Properties* (eds. Page, A. L., Miller, R. H. & Keeney, D. R.) 403–430  
670 (American Society of Agronomy and Soil Science Society of America, Madison, WI, 1982).
- 671 51. Anderson, J. P. E. & Domsch, K. H. A physiological method for the quantitative  
672 measurement of microbial biomass in soils. *Soil Biol Biochem* 10, 215–221 (1978).
- 673 52. Scheu, S. Automated measurement of the respiratory response of soil microcompartments:  
674 Active microbial biomass in earthworm faeces. *Soil Biol Biochem* 24, 1113–1118 (1992).
- 675 53. Breiman, L. Random forests. *Mach Learn* 45, 5–32 (2001).

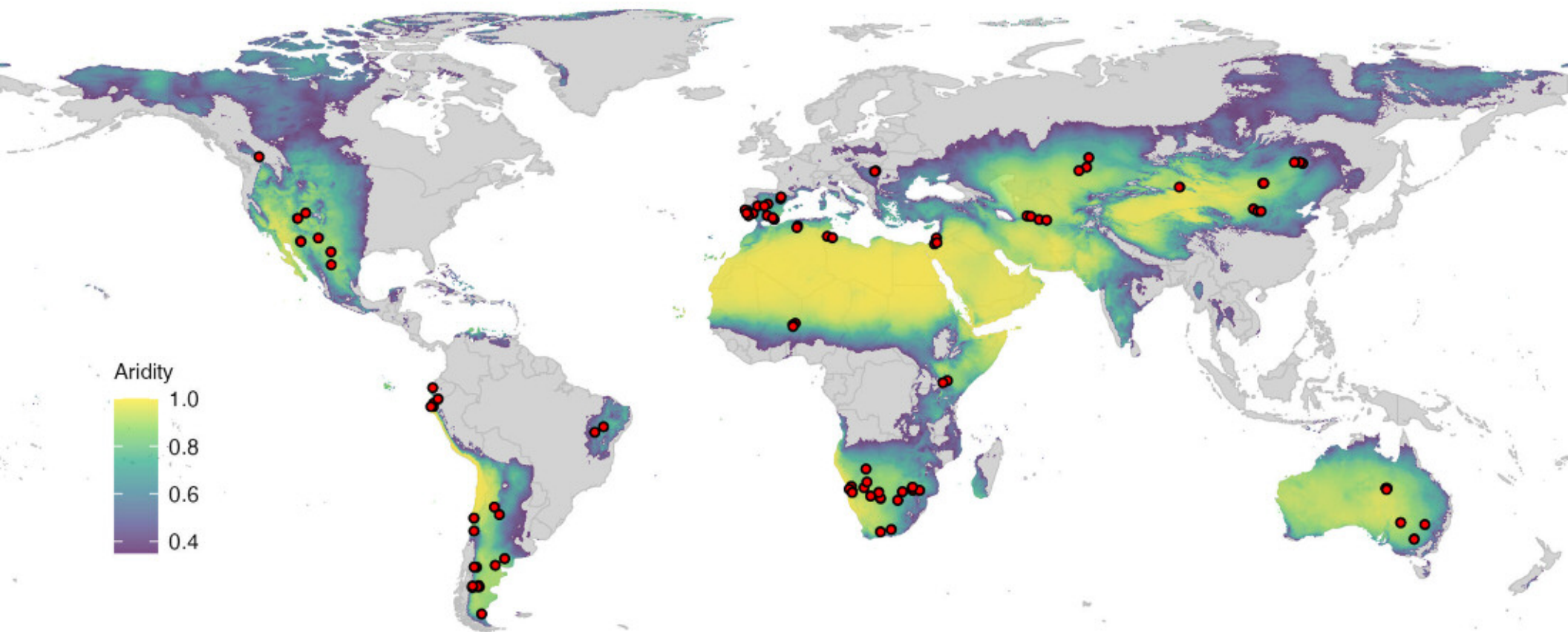
- 676 54. Gelman, A. Scaling regression inputs by dividing by two standard deviations. *Stat Med* 27,  
677 2865–2873 (2008).
- 678 55. Kuznetsova, A., Brockhoff, P. B. & Christensen, R. H. B. lmerTest package: Tests in linear  
679 mixed effects models. *J Stat Softw* 82, 1–26 (2017).
- 680 56. James, G., Witten, D., Hastie, T. & Tibshirani, R. An Introduction to Statistical Learning.  
681 vol. 112 (Springer, 2013).
- 682 57. R Core Team. R: A Language and Environment for Statistical Computing. Preprint at  
683 <https://www.R-project.org/> (2023).
- 684 58. Gelman, A. & Su, Y.-S. arm: Data Analysis Using Regression and Multilevel/Hierarchical  
685 Models. Preprint at <https://CRAN.R-project.org/package=arm> (2022).
- 686 59. Wickham, H. Ggplot2: Elegant Graphics for Data Analysis. (Springer-Verlag New York,  
687 2016).
- 688 60. Bates, D., Mächler, M., Bolker, B. M. & Walker, S. C. Fitting linear mixed-effects models  
689 using lme4. *J Stat Softw* 67, 1–48 (2015).
- 690 61. Stoffel, M. A., Nakagawa, S. & Schielzeth, H. partR2: Partitioning R2 in generalized linear  
691 mixed models. *bioRxiv* (2020) doi:10.1101/2020.07.26.221168.
- 692 62. Pedersen, T. L. patchwork: The Composer of Plots. R package version 1.1.1.  
693 <https://CRAN.R-project.org/package=patchwork>. Preprint at [https://cran.r-](https://cran.r-project.org/package=patchwork)  
694 [project.org/package=patchwork](https://cran.r-project.org/package=patchwork) (2020).
- 695 63. Massicotte, P. & South, A. rnaturalearth: World Map Data from Natural Earth. Preprint at  
696 <https://CRAN.R-project.org/package=rnaturalearth> (2023).
- 697 64. Liaw, A. & Wiener, M. Classification and Regression by randomForest. *R News* 2, 18–22  
698 (2002).
- 699 65. Pebesma, E. & Bivand, R. Spatial Data Science: With Applications in R. (Chapman and  
700 Hall/CRC, 2023).
- 701 66. Hijmans, R. J. terra: Spatial Data Analysis. Preprint at [https://CRAN.R-](https://CRAN.R-project.org/package=terra)  
702 [project.org/package=terra](https://CRAN.R-project.org/package=terra) (2023).
- 703 67. Garnier, S. viridis: Default Color Maps from ‘matplotlib’. Preprint at [https://cran.r-](https://cran.r-project.org/package=viridis)  
704 [project.org/package=viridis](https://cran.r-project.org/package=viridis) (2018).

705 68. Díaz-Martínez, P, Maestre, F.T., Moreno-Jiménez, E. & Plaza, C. Data from Vulnerability of  
706 mineral-associated soil organic carbon to climate in global drylands. Figshare.  
707 <https://doi.org/10.6084/m9.figshare.24678891> (2024).

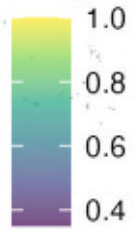








Aridity



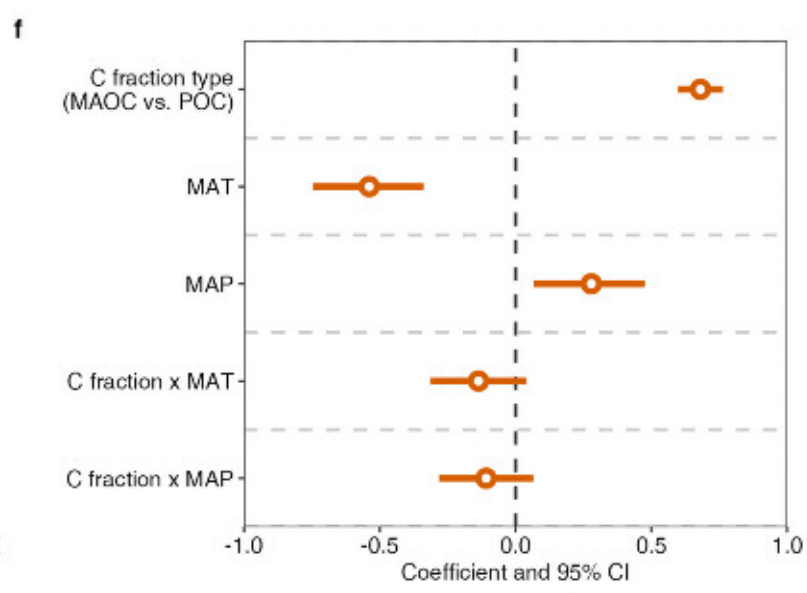
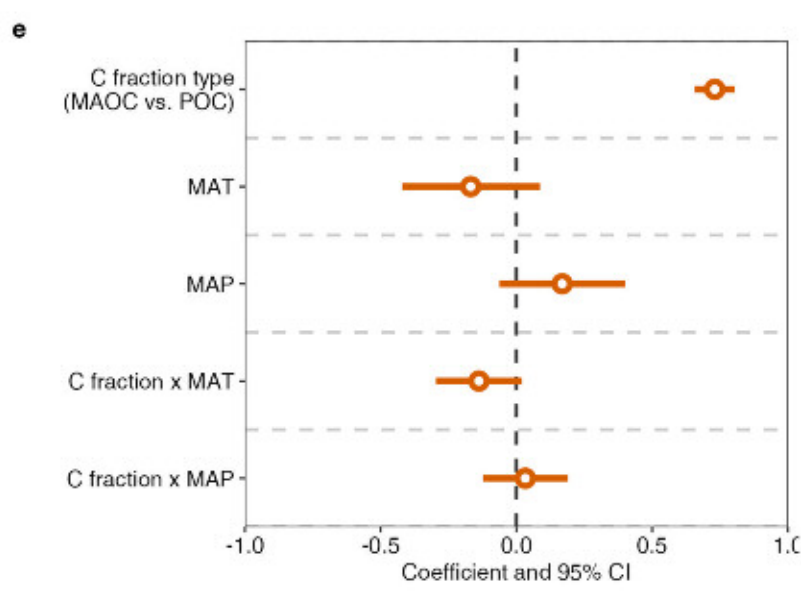
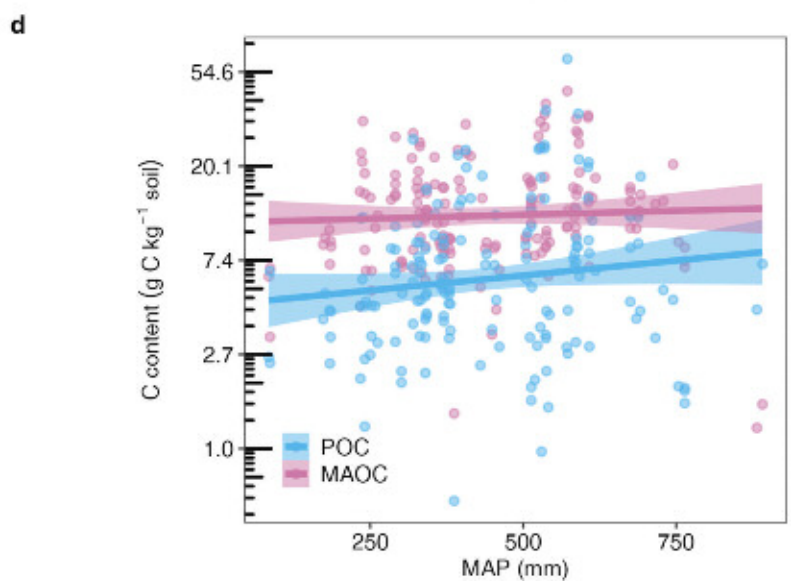
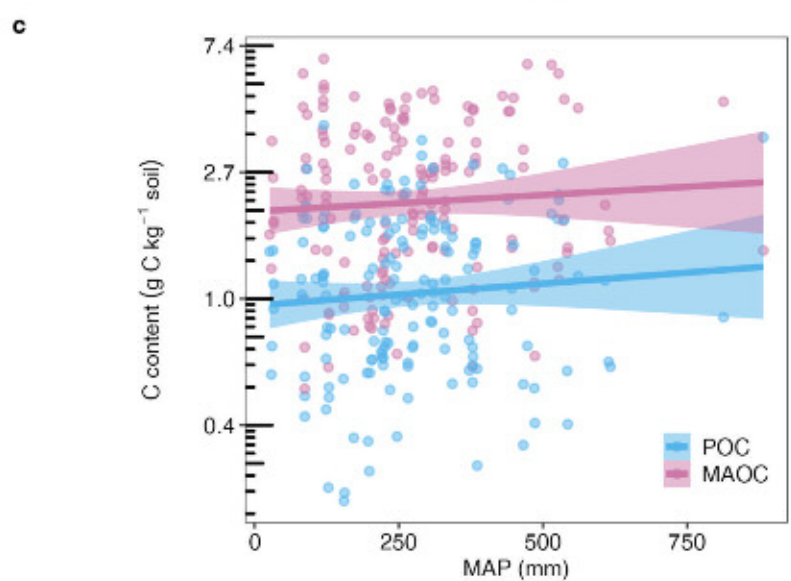
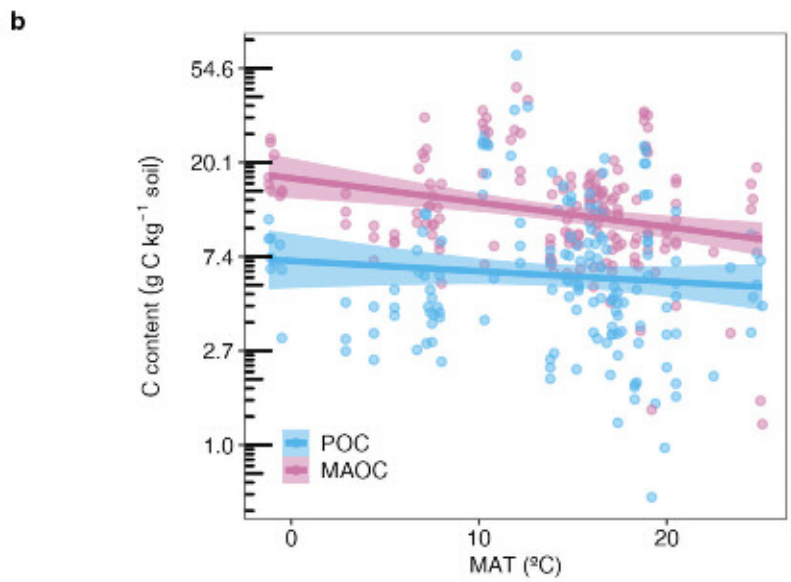
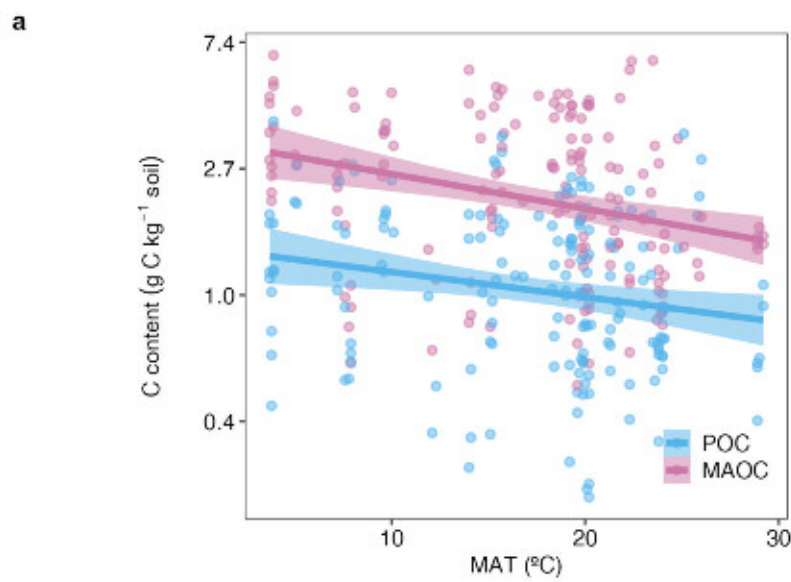
1.0

0.8

0.6

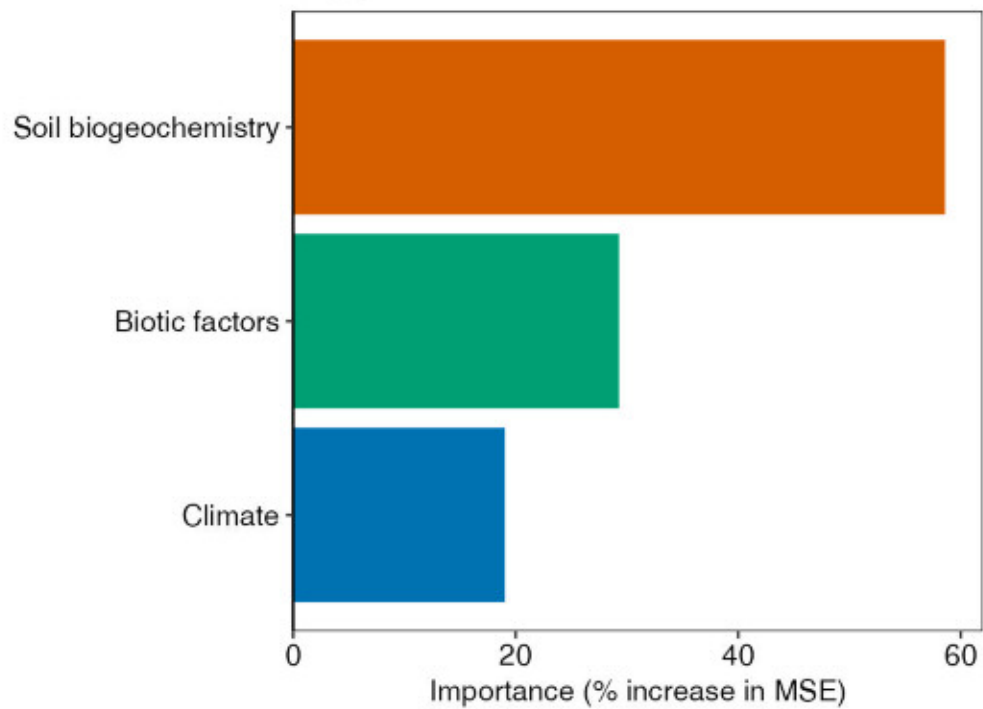
0.4



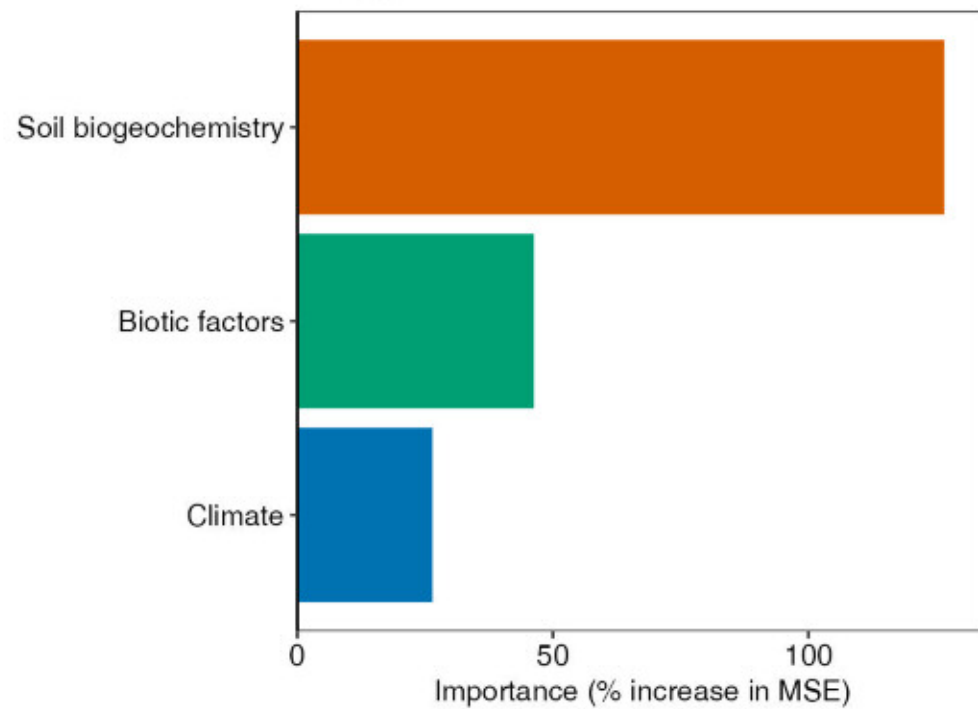


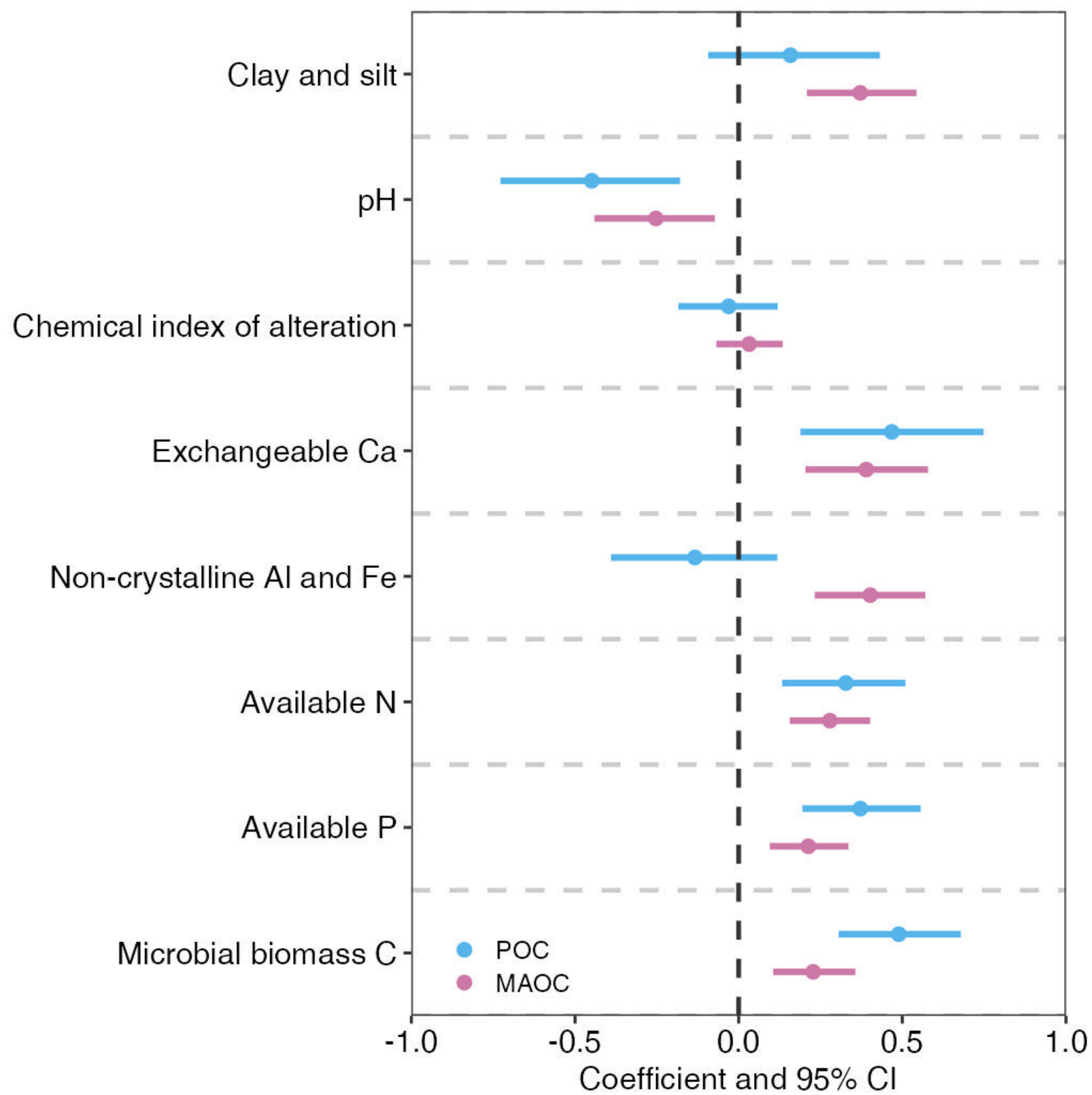


POC



MAOC





<b>Variable</b>	<b>n</b>	<b>Min</b>	<b>Q1</b>	<b>Median</b>	<b>Mean</b>	<b>Q3</b>	<b>Max</b>
MAT (°C)	326	-1.2	10.4	16.6	15.5	19.9	29.2
MAP (mm)	326	26	233	332	357	505	891
Net primary productivity (NDVI, unitless)	326	0.06	0.13	0.17	0.19	0.25	0.43
Woody cover (%)	326	0	15	46	48	83	100
Plant richness (number of species)	326	0	8	16	19	26	57
Herbivore richness (number of species)	326	0	1	2	2	3	6
Clay and silt (g kg <sup>-1</sup> )	326	10	120	271	325	512	870
pH	326	4.5	6.1	7.0	6.9	7.8	9.9
Chemical index of alteration (%)	326	42	74	81	79	87	97
Exchangeable Ca (mg kg <sup>-1</sup> )	321	39	843	1730	3394	3443	42446
Non-crystalline Al and Fe (mg kg <sup>-1</sup> )	326	28	475	932	1357	1620	9889
Available N (mg kg <sup>-1</sup> )	326	1	8	14	21	26	143
Available P (mg kg <sup>-1</sup> )	323	0.1	5.5	11.5	13.6	17.8	87.6
Microbial biomass C (mg kg <sup>-1</sup> )	326	16	101	186	245	331	1065

<b>Variable</b>	<b>Category</b>	<b>Number of observations</b>
Vegetation type	Grassland	94
	Shrubland	160
	Forest	72
Grazing pressure	Zero	43
	Low	88
	Medium	97
	High	98